Reprinted from the Journal of the American Chemical Society, 1993, 115.

Synthesis, Characterization, and Thermodynamic Analysis of a 1 + 1 Self-Assembling Structure Based on the Cyanuric Acid·Melamine Lattice

Christopher T. Seto and George M. Whitesides*

Contribution from the Department of Chemistry, Harvard University, Cambridge, Massachusetts 02138. *Received August 7, 1992*

Abstract: This article describes the reaction of the trivalent melamine derivative C_6H_3-1,3,5-$[CO_2(CH_2)_4OCOC_6H_4$-2-$NHC_3N_3(NH_2)(NHCH_2CH_2C(CH_3)_3)]_3$ (homoflexM$_3$, *h*-flexM$_3$) with the trivalent isocyanurate derivative C_6H_3-1,3,5-$[CONHC_6H_4$-3-$N((CH_2)_{17}CH_3)COC_6H_3$-2-$NC(O)NHC(O)NHC(O)$-5-$O(CH_2)_{17}CH_3]_3$ (hubCA$_3$) in $CHCl_3$ to afford a structurally well-defined 1 + 1 supramolecular aggregate *h*-flexM$_3$·hubCA$_3$. This structure is held together by a network of 18 hydrogen bonds and is one of the most stable nonbiological supramolecular aggregates synthesized to date. The structure was characterized by ^{1}H NMR and UV spectroscopies, gel permeation chromatography, and vapor pressure osmometry. The exchange reaction between *h*-flexM$_3$·hubCA$_3$ and C_6H_3-1,3,5-$[CO_2(CH_2)_4OCOC_6H_3$-2-$NHC_3N_3(NH_2)(NHCH_2CH_2C(CH_3)_3)$-5-$CH_3]_3$ (*h*-flexM′$_3$, a close structural analog of *h*-flexM$_3$) was monitored by ^{1}H NMR spectroscopy. This exchange reaction appeared to occur by dissociation; the reaction was first-order in *h*-flexM$_3$·hubCA$_3$ and zero-order in *h*-flexM′$_3$. The transition-state parameters, $\Delta H^{\ddagger} = 24 \pm 2$ kcal/mol, $\Delta S^{\ddagger} = -6 \pm 12$ eu, and $\Delta G^{\ddagger} = 26 \pm 6$ kcal/mol, for the exchange reaction were calculated by following the exchange process at several temperatures. These thermodynamic data indicated that the average enthalpy per hydrogen bond in this system was 1.3 ± 0.1 kcal/mol. Several mechanisms by which the exchange reaction may occur have been postulated and discussed.

Introduction

We are developing the methodology to construct large, soluble, self-assembling structures that are based on the hydrogen-bonded complex between cyanuric acid and melamine (CA·M).[1-4] We have used the cyclic hexameric motif (CA$_3$·M$_3$) that is formed from three melamine and three isocyanuric acid molecules as the core for these self-assembling molecular aggregates. To understand the thermodynamics of formation of these structures and to estimate the strength of the array of 18 hydrogen bonds that hold the cyclic hexamer together, we have constructed a prototypical system in which a tris melamine (homoflexM$_3$, *h*-flexM$_3$) and a tris isocyanuric acid (hubCA$_3$) associate to form the stable, structurally well-defined 1 + 1 molecular aggregate *h*-flexM$_3$·hubCA$_3$.[5] This article reports the transition-state parameters $\Delta H^{\ddagger}$, $\Delta S^{\ddagger}$, and $\Delta G^{\ddagger}$ that are associated with the exchange reaction between preformed *h*-flexM$_3$·hubCA$_3$ and free *h*-flexM′$_3$ (a close structural analog of *h*-flexM$_3$) (Scheme I).

Design of the *h*-flexM$_3$·hubCA$_3$ Binding System. Previous self-assembling aggregates based on the CA$_3$·M$_3$ unit have contained four or five particles.[1] The thermodynamics of formation in these systems is difficult to analyze because they involve multiple binding sites and because they display positive cooperativity in their formation. We have designed the binding system *h*-flexM$_3$·hubCA$_3$ so that only two molecules assemble to form the cyclic hexameric structure. This 1 + 1 system should be the least complicated of the aggregates built from the CA·M lattice and should provide a tractable system with which to investigate the thermodynamics of formation of self-assembling aggregates.

Scheme I. Exchange of *h*-flexM$_3$ for *h*-flexM′$_3$ in the *h*-flexM$_3$·hubCA$_3$ Complex[a]

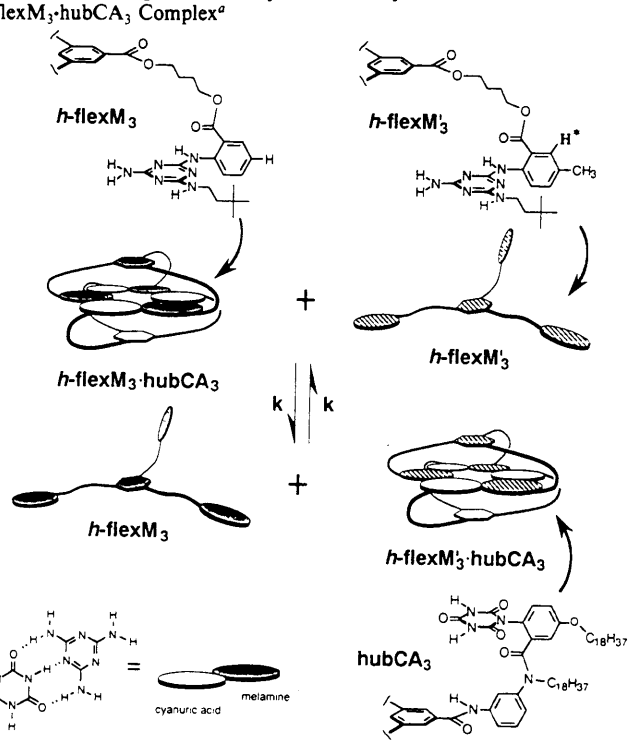

[a] *h*-flexM$_3$ and *h*-flexM′$_3$ differ by a CH_3 group. H* indicates the proton of *h*-flexM′$_3$ that was monitored in the *h*-flexM′$_3$·hubCA$_3$ complex by ^{1}H NMR spectroscopy. This proton has a different resonance in *h*-flexM′$_3$·hubCA$_3$ and free *h*-flexM′$_3$.

Structure of hubCA$_3$ and *h*-flexM$_3$. We constructed hubCA$_3$ and *h*-flexM$_3$ by covalently linking three CA units (and three M units) to a central "hub" using "spokes" that are compatible with the geometry necessary to form the desired hydrogen-bonding network. The spokes of hubCA$_3$ consist of rigid aromatic spacers connected through amide bonds that preorganize the molecule for complexation and reduce the loss of conformational entropy associated with assembly. (The six C_{18} chains were incorporated in the structure in an unsuccessful attempt to make uncomplexed hubCA$_3$ soluble in chloroform.) We constructed *h*-flexM$_3$ with

(1) Seto, C. T.; Whitesides, G. M. *J. Am. Chem. Soc.* **1990**, *112*, 6409. Seto, C. T.; Whitesides, G. M. *J. Am. Chem. Soc.* **1991**, *113*, 712. Seto, C. T.; Whitesides, G. M. *J. Am. Chem. Soc.*, in press.

(2) Seto, C. T.; Mathias, J. P.; Whitesides, G. M. *J. Am. Chem. Soc.*, in press.

(3) Whitesides, G. M.; Mathias, J. P.; Seto, C. T. *Science* **1991**, *254*, 1312.

(4) For a thermodynamic analysis of another artificial binding system, see: Smithrud, D. B.; Wyman, T. B.; Diederich, F. *J. Am. Chem. Soc.* **1991**, *113*, 5420.

(5) We have reported previously that the flexible tris melamine flexM$_3$ reacts with 3 equiv of alkyl isocyanurate to give a stable complex. The "spokes" of the tris melamine that we describe in this article are one methylene unit longer than the "spokes" of flexM$_3$, and thus we have called the tris melamine described here homoflexM$_3$ or *h*-flexM$_3$. See Scheme I for the structure of *h*-flexM$_3$.

0002-7863/93/1515-1330$04.00/0

Scheme II. Synthesis of hubCA$_3$[a]

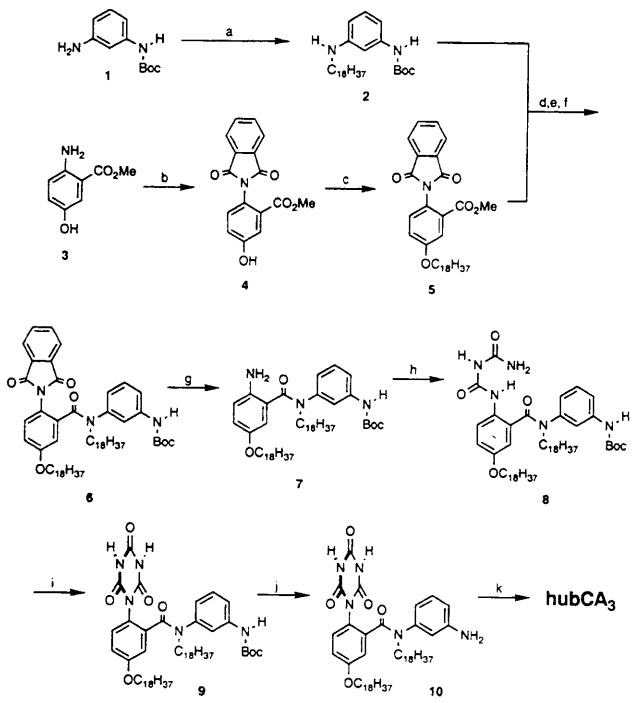

[a] Reagents: (a) $C_{18}H_{37}Br$, DMF, 115 °C, 52%; (b) *o*-phthaloyl dichloride, THF, 0 °C, 62%; (c) $C_{18}H_{37}Br$, K_2CO_3, 18-crown-6, DMF, 80 °C, 89%; (d) NaOH, H_2O, THF, 25 °C; (e) $SOCl_2$, reflux; (f) Et_3N, CH_2Cl_2, 25 °C, 91% (3 steps); (g) H_2NNH_2, MeOH, reflux; (h) nitrobiuret, H_2O, reflux, 86% (2 steps); (i) 1,1′-carbonyldiimidazole, *t*-BuOK, THF, 25 °C, 70%; (j) F_3CCO_2H, CH_2Cl_2, 25 °C, 87%; (k) 1,3,5-$C_6H_3(COCl)_3$ (0.33 equiv), CH_2Cl_2, 0 °C, 91%.

flexible spokes that allow the molecule to settle into the geometry that maximizes the strength of the hydrogen-bonding interactions between *h*-flexM$_3$ and hubCA$_3$, without introducing strain into the complex.

Thermodynamics of the Formation of *h*-flexM$_3$·hubCA$_3$. A. Difficulty in Measuring $\Delta G_{formation}$. We have not been able to measure the equilibrium binding constant between hubCA$_3$ and *h*-flexM$_3$ using standard analytical techniques. The binding constant is too large to measure by ^{1}H NMR spectroscopy. The complex is stable at concentrations as low as 10 μM, and at this concentration we did not observe any resonances corresponding to either free *h*-flexM$_3$ or free hubCA$_3$. There is no significant shift in the resonances of the hydrogen-bonded protons of the components that would indicate weakening or breaking of the hydrogen-bonded network.[6] The changes that occur in the UV and fluorescence spectra of hubCA$_3$ and *h*-flexM$_3$ upon binding are not large enough to be useful in measuring the association constant between these molecules.

The most straightforward method (conceptually) to measure thermodynamic parameters for formation of a complex is to study the reaction of the components calorimetrically. This method seems closed to us: hubCA$_3$ is virtually insoluble in the solvents of greatest interest, and *h*-flexM$_3$ is strongly associated by intermolecular hydrogen bonds. We have, instead, turned to an indirect method based on an exchange reaction.

B. Transition-State Parameters for Exchange between *h*-flexM$_3$·hubCA$_3$ and *h*-flexM′$_3$. We have measured the thermodynamic parameters that are associated with the transition state for the exchange between *h*-flexM$_3$·hubCA$_3$ and free *h*-flexM′$_3$ (Scheme I). This interchange process appears to occur by dissociation. On the basis of its thermodynamics, we infer (with some assumptions) the corresponding parameters for association of the components.

(6) We should be able to detect a minimum of 10% dissociated species in the ^{1}H NMR spectrum of *h*-flexM$_3$·hubCA$_3$ at 10 μM concentration. Since we do not observe any dissociated species, $K_{association} \geq [h\text{-flexM}_3\cdot\text{hubCA}_3]/[\text{hubCA}_3][h\text{-flexM}_3] \geq (9 \times 10^{-6})/(10^{-6})^2 \geq 9 \times 10^6$ M^{-1}, corresponding to a $\Delta G_{formation} \leq -9.5$ kcal/mol.

Scheme III. Synthesis of *h*-flexM$_3$ and *h*-flexM′$_3$[a]

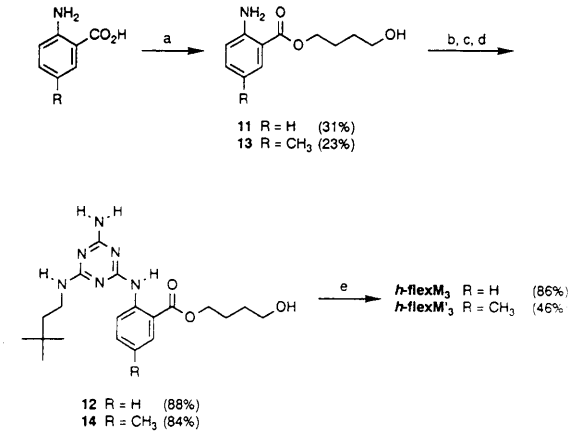

[a] Reagents: (a) H^+ (*p*-toluenesulfonic acid, R = H; methanesulfonic acid, R = CH_3), $HO(CH_2)_4OH$, toluene, reflux; (b) cyanuric chloride, THF, 0 °C; (c) NH_3, THF, 0 °C; (d) $H_2N(CH_2)_2C(CH_3)_3$, THF, reflux; (e) 1,3,5-$C_6H_3(COCl)_3$ (0.33 equiv), THF, 25 °C.

Scheme IV. Schematic Diagram of the Four Possible Geometrical Isomers of *h*-flexM$_3$·hubCA$_3$[a]

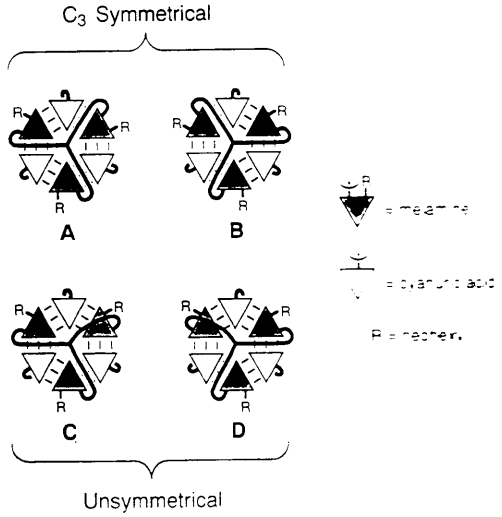

[a] This is a view from the top of the complex with the hub and spokes of *h*-flexM$_3$ facing the reader and those of hubCA$_3$ extending below the plane of the page. The hub and spokes of hubCA$_3$ have been truncated for the sake of clarity.

Results

Synthesis of hubCA$_3$, *h*-flexM$_3$, and *h*-flexM′$_3$. The synthesis of these compounds is outlined in Schemes II and III. *h*-flexM$_3$ and *h*-flexM′$_3$ differ only by a single methyl group on each spoke.

Preparation of the *h*-flexM$_3$·hubCA$_3$ Complex. A. Solubility and Equilibration. We prepared *h*-flexM$_3$·hubCA$_3$ by mixing equimolar amounts of the two components in chloroform and aging the sample for ~16 h at room temperature. hubCA$_3$ alone has a low solubility in chloroform (≤10 μM). During the first 3–4 h of the aging process, the hubCA$_3$, which is initially present in the solution as a suspension, dissolves and forms *h*-flexM$_3$·hubCA$_3$. *h*-flexM$_3$ solubilizes up to, but not more than, 1 equiv of hubCA$_3$. This result provides qualitative evidence that the stoichiometry of the complex is 1:1.

B. Symmetrical and Unsymmetrical Complexes. There are two different substituents attached to the M units of *h*-flexM$_3$, and *h*-flexM$_3$·hubCA$_3$ can exist as four possible geometrical isomers (Scheme IV). Enantiomers A and B are C_3-symmetrical structures, and enantiomers C and D are unsymmetrical (C_1). ^{1}H NMR spectroscopy demonstrates that the most stable form of *h*-flexM$_3$·hubCA$_3$ is a C_3-symmetrical structure: we observe only

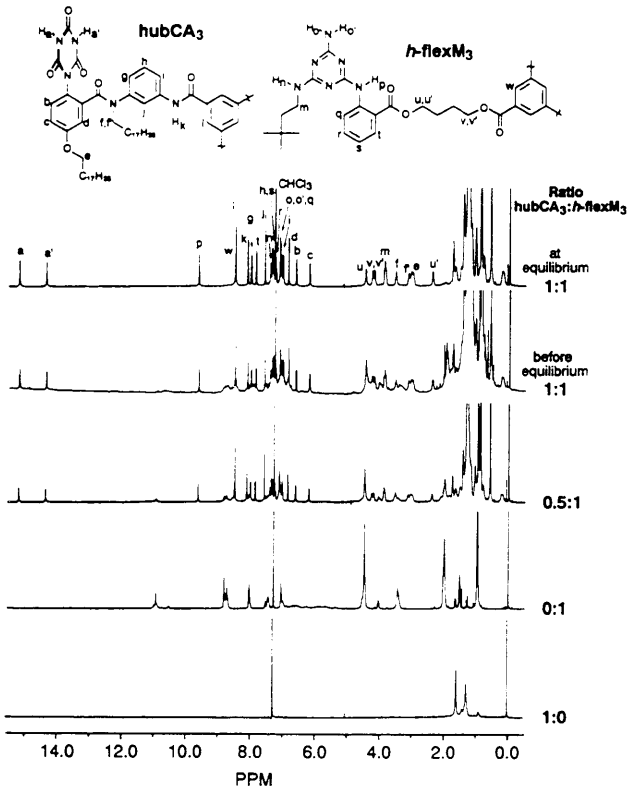

Figure 1. ^1H NMR spectra of *h*-flexM_3·hubCA_3, free *h*-flexM_3, and free hubCA_3 (500 MHz, $CDCl_3$). The probable peak assignments are shown at the top of the figure. The spectrum of *h*-flexM_3·hubCA_3 before equilibrium was recorded approximately 2 h after the components were mixed in $CDCl_3$.

one set of resonances for each of the three spokes of hubCA_3 and of *h*-flexM_3.

The initial complex that is formed upon combining hubCA_3 and *h*-flexM_3 is a mixture of compounds. On the basis of gel permeation chromatography (GPC) and ^1H NMR spectroscopy measurements, we believe that it contains a mixture of symmetrical and unsymmetrical complexes and, possibly, aggregates having a stoichiometry different than 1:1. Over a period of ~16 h (at room temperature), all of these species isomerize to the most stable, C_3-symmetrical structure.

Characterization of *h*-flexM_3·hubCA_3. A. ^1H NMR Spectroscopy. The ^1H NMR spectra of *h*-flexM_3·hubCA_3, free hubCA_3, and free *h*-flexM_3 are shown in Figure 1. The only distinguishable resonances in the spectrum of free hubCA_3 at saturation in $CDCl_3$ originate in the protons of the C_{18} chains. The spectrum of hubCA_3 and *h*-flexM_3 at a ratio of 0.5:1 illustrates that exchange of *h*-flexM_3·hubCA_3 with excess *h*-flexM_3 is slow on the NMR time scale; we observe separate resonances for each of these species. The spectrum also shows that this mixture contains only fully formed *h*-flexM_3·hubCA_3 and free *h*-flexM_3, and does not contain aggregates of hubCA_3 and *h*-flexM_3 that have stoichiometries other than 1:1.

Figure 1 also shows a spectrum of *h*-flexM_3·hubCA_3 before the complex has fully equilibrated to the C_3-symmetrical structure. This spectrum was recorded before all of the hubCA_3 in the sample had been solubilized. The spectrum thus resembles that of *h*-flexM_3·hubCA_3 at the 0.5:1 stoichiometry. There are also other resonances in this spectrum that we believe correspond to unsymmetrical isomers. These peaks disappear as the complex equilibrates to the symmetrical structure.

B. Characteristic Features of the Spectrum of *h*-flexM_3·hubCA_3. The probable peak assignments for *h*-flexM_3·hubCA_3 are shown at the top of Figure 1. Several methylene protons of hubCA_3 (f,f') and *h*-flexM_3 (u,u' and v,v') become diastereotopic in the 1:1 complex and appear as separate resonances. The imide protons (a,a') of hubCA_3 occupy different hydrogen-bonding sites in the complex and thus appear as separate resonances.

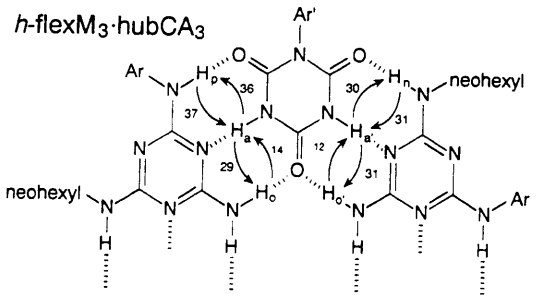

Figure 2. Percent intermolecular NOEs among the hydrogen-bonded protons in *h*-flexM_3·hubCA_3.

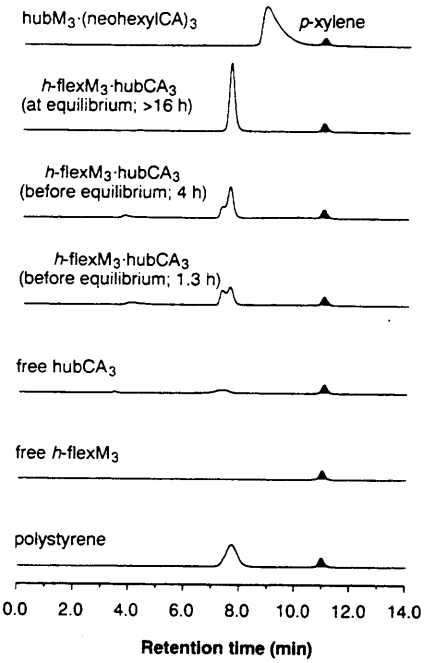

Figure 3. Gel permeation chromatograms of free and complexed *h*-flexM_3 and hubCA_3 eluted with chloroform. The two chromatograms that are designated "before equilibrium" illustrate the equilibration of the initially formed 1:1 complex to the C_3-symmetrical form; 1.3 and 4 h refer to the time between initial mixing of the components and the time that the chromatogram was recorded, respectively. The small peak at 11 min is *p*-xylene used as an internal standard. The bottom trace shows polystyrene (av MW 5050; polydispersity = 1.05) for reference. The top chromatogram is that of the tris melamine derivative hubM_3 complexed with 3 equiv of neohexyl isocyanurate and is included to illustrate tailing of peaks in less stable complexes.

We examined *h*-flexM_3·hubCA_3 by ^1H NMR spectroscopy in the mixed solvents methanol/chloroform and DMSO/chloroform. These are hydrogen-bonding solvent systems that destabilize the aggregate. In 20% methanol/chloroform, the aggregate dissociated over a period of ~3 days to give an equilibrium mixture that contained ~5% *h*-flexM_3·hubCA_3 and ~95% dissociated species. In 15% DMSO/chloroform, the aggregate completely dissociated into free *h*-flexM_3 and free hubCA_3 over a period of ~12 h. These results indicate that *h*-flexM_3·hubCA_3 is the most stable hydrogen-bonded aggregate that we have made and is one of the most stable, nonbiological hydrogen-bonded aggregates now known.

C. Nuclear Overhauser Effects. We observe strong NOEs among the hydrogen-bonding protons of hubCA_3 and *h*-flexM_3, because these protons are held in close proximity (~2.5 Å) in *h*-flexM_3·hubCA_3. The results are summarized in Figure 2.

D. Gel Permeation Chromatography. The GPC traces of *h*-flexM_3·hubCA_3 and its components are shown in Figure 3.[7] The trace of free *h*-flexM_3 shows no defined peaks because this compound is self-associated in chloroform solution and probably exists

(7) GPC separates molecules according to hydrodynamic radii. Shorter retention times correspond to higher molecular weights.

Scheme V. Possible Structures for the Aggregate with a 7.2-min Retention Time in GPC: Incomplete Networks of Hydrogen Bonds and Dimers

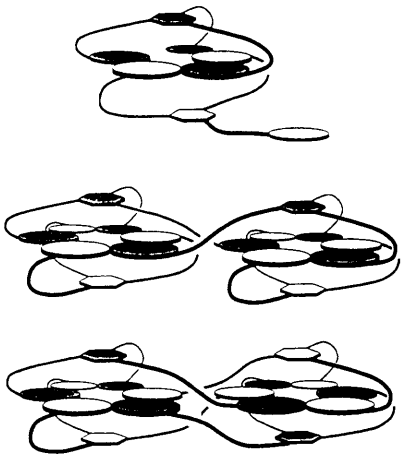

as a variety of oligomers with a broad distribution of molecular weights. The trace of $hubCA_3$ (at saturation in chloroform) shows a small, broad peak at 7.2 min, suggesting that this compound may exist partially as a dimer in solution. In contrast, the GPC trace of *h*-flexM_3·hubCA_3 shows a single, sharp peak at 7.5 min corresponding to the complex. The absence of tailing in this chromatogram shows that the 1 + 1 complex is stable in chloroform solution over the time scale of the GPC analysis.[8] The top trace shows the chromatogram of a hydrogen-bonded complex that is less stable than *h*-flexM_3·hubCA_3 (a tris melamine derivative complexed with 3 equiv of neohexyl isocyanurate). The peak corresponding to this complex shows considerable tailing caused by dissociation of the aggregate on the GPC column. The trace of the polystyrene standard is included for reference.

Retention times in GPC are roughly proportional to the logarithm of the molecular weight of a molecule.[8] Using this relationship and a variety of other hydrogen-bonded aggregates as standards,[1,2] we estimate that a peak with a retention time of 7.5 min corresponds to a species with a molecular weight of ~5200 Da. This value is higher than the calculated molecular weight of *h*-flexM_3·hubCA_3 (4101 Da). The six C_{18} chains on this complex may cause it to interact differently with the GPC matrix than the other hydrogen-bonded aggregates that we have used as standards.

We can use GPC to monitor the equilibration of initially formed *h*-flexM_3·hubCA_3 to the C_3-symmetrical structure. Figure 3 shows two GPC traces of the complex before it has reached equilibrium. The trace that was recorded at 1.3 h after the components were mixed shows two peaks at 7.2 and 7.5 min. As the mixture equilibrates, the peak at 7.2 min disappears, and the peak at 7.5 min increases in intensity until it is the only discernible peak in the chromatogram (other than the reference). We have two possible explanations for the peak at 7.2 min. This peak may correspond to unsymmetrical isomers of *h*-flexM_3·hubCA_3 or an incompletely formed 1 + 1 complex.[9] Alternately, the peak could correspond to dimers or other oligomers of the 1 + 1 aggregate. (Scheme V shows a possible structure for a 1:1 complex with an incomplete network of hydrogen bonds and two possible structures for a dimer.) On the basis of the relationship between retention time and molecular weight mentioned above, we expect that a peak at 7.2 min would have a MW of ~5600 Da; a dimer (MW = 8202) of *h*-flexM_3·hubCA_3 would have a retention time of ~5.8 min. These estimates indicate that the peak at 7.2 min probably does not correspond to a dimer.

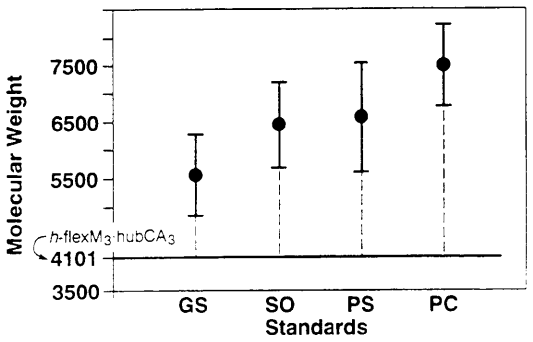

Figure 4. Experimental molecular weight of *h*-flexM_3·hubCA_3 determined by vapor pressure osmometry using four different molecular weight standards. The solid horizontal line corresponds to the calculated MW of *h*-flexM_3·hubCA_3. The four MW standards were GS = *N,N'*-bis(*t*-Boc)gramicidin S (MW 1342), SO = sucrose octaacetate (MW 679), PS = polystyrene (average MW 5050, polydispersity = 1.05), and PC = perbenzoyl β-cyclodextrin (MW 3321). The error bars correspond to the sum of the standard deviations of the VPO measurements of the standard and unknown. These experiments were performed at 37 °C in $CHCl_3$ over the concentration range 2–16 mM complex.

In both of the traces of *h*-flexM_3·hubCA_3 before it has reached equilibrium, there is a small, broad peak at 3.8 min. This peak corresponds to a species (or mixture of species) with a MW larger than 30 kDa (the upper MW limit of our GPC column) and may be caused by oligomeric $hubCA_3$ that has not yet complexed with *h*-flexM_3. This high MW peak also disappears during the equilibration process.

E. Vapor Pressure Osmometry (VPO). We have determined the molecular weight of *h*-flexM_3·hubCA_3 by VPO (Figure 4). Using a variety of molecular weight standards, the experimental molecular weight for the 1 + 1 complex ranges from 35 to 80% higher than the calculated value. This result follows the same trend that we have observed before.[2] Many of these hydrogen-bonded self-assembling aggregates give molecular weights, as determined by VPO, that are higher than the calculated values. Certainly it seems possible that *h*-flexM_3·hubCA_3 may undergo weak, nonspecific intercomplex association or repulsion that is not evident by ^1H NMR analysis. The deviations of the estimated from the expected values of molecular weight are, however, the largest we have observed in this class of self-assembling complexes. Since this complex is particularly stable, and since the deviation from the expected value is large, we have examined the context of these VPO results in some detail.

Figure 5 illustrates the concentration dependence of VPO results for four molecular weight standards (bottom graph) and five hydrogen-bonded aggregates[1,2] (top graph). If all of the compounds behaved ideally, all of the data for each compound would lie on a line with a slope of zero. Instead, the different standards and aggregates each give lines that have different slopes and different *y*-intercepts. The sucrose octaacetate and perbenzoyl β-cyclodextrin standards give lines with slopes that are close to zero. These compounds seem to behave as ideal solutes. The gramicidin standard gives a line with a negative slope: this is the result that is expected if this compound self-associates in a concentration-dependent manner. This observation is consistent with the molecular structure of gramicidin, which is a cyclic decapeptide with many sites for hydrogen bonding. Polystyrene gives a line with a positive slope. As the concentration increases, the polystyrene molecules seem to repel one another, a result that may be caused by the unfavorability of compressing a random coil. The data for *h*-flexM_3·hubCA_3 appear at lower values of $\Delta V/C$ than any of the other compounds, showing that the molecular weight of this aggregate sensed by VPO is higher than the calculated value; that is, the number of particles sensed (as reflected by the influence of this compound on the vapor pressure) is smaller than the number expected from its postulated structure. We do not have an explanation for this result in which we are confident.

(8) Stable complexes give sharp, symmetrical peaks in GPC, while less stable complexes show tailing of their peaks caused by decomplexation during the analysis. Stevens, F. J. *Biochemistry* **1986**, *25*, 981. Stevens, F. J. *Biophys. J.* **1989**, *55*, 1155.

(9) We do not understand why the symmetrical and unsymmetrical isomers of *h*-flexM_3·hubCA_3 would have different retention times, since both isomers have the same MW. One plausible explanation is that the isomers have different geometries, causing the symmetrical and unsymmetrical isomers to interact differently with the GPC matrix.

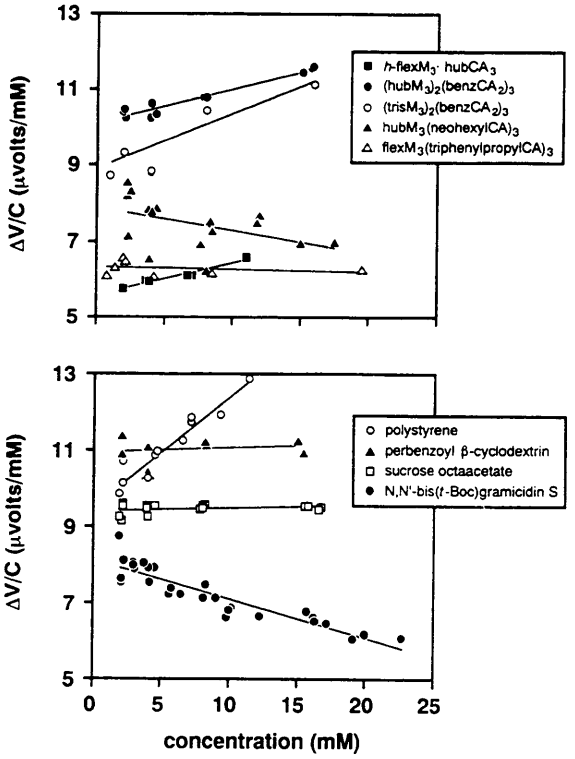

Figure 5. Plots showing the concentration dependence of data from vapor pressure osmometry (chloroform, 37 °C) for five hydrogen-bonded supramolecular complexes (top graph) and four molecular weight standards (bottom graph). ΔV is the difference in the voltage that is measured by the osmometer when pure solvent on the thermister bead is replaced by a solution with a concentration of $[C]$. This difference in voltage is proportional to the difference in vapor pressure between pure solvent and the solution with concentration $[C]$ and, thus, is also proportional to the concentration of particles in the solution that is sensed by VPO. The lines correspond to a least-squares analysis of the data.

All of the other data suggest that the 1:1 complex is, in fact, particularly stable; these data are consistent with the postulated structure. We hypothesize that the C_{18} chains of *h*-flexM$_3$·hubCA$_3$ lie at the origin of the difference between this complex and the others we have examined. Association of C_{18} chains *between* 1:1 complexes would, for example, cause deviations in $\Delta V/C$ in the observed direction. The positive slope of the line could be caused by unfavorable compression of the six C_{18} chains at higher concentrations.

Hydrogen-bonded aggregates with similar molecular structures behave similarly in VPO analysis. The structures that incorporate a tris melamine complexed with 3 equiv of mono isocyanuric acid (1 + 3 complexes; triangles, top graph) have similar slopes and positions on the graph. The structures that incorporate 2 equiv of a tris melamine and 3 equiv of a bis isocyanuric acid (2 + 3 complexes; circles) also behave similarly. The tris melamine portion of *h*-flexM$_3$·hubCA$_3$ and flexM$_3$(triphenylpropylCA)$_3$ are similar, and both aggregates give molecular weights, as determined by VPO, that are higher than the calculated values.[1] Figure 5 indicates that molecular weights derived from VPO depend strongly on the choice of standard. Use of several standards may make it possible to identify types of nonideal behavior for an unknown.

In summary, although our analysis of the structure of *h*-flexM$_3$·hubCA$_3$ is based on inference, the results are consistent with our investigations of other self-assembled structures based on the CA·M lattice.[1,2,10]

Exchange between *h*-flexM$_3$·hubCA$_3$ and *h*-flexM′$_3$. We measured the rate of exchange between preformed *h*-flexM$_3$·hubCA$_3$ and free *h*-flexM′$_3$ by following the appearance of the resonance for H* (Scheme I) of *h*-flexM′$_3$·hubCA$_3$ using ^{1}H NMR spectroscopy.

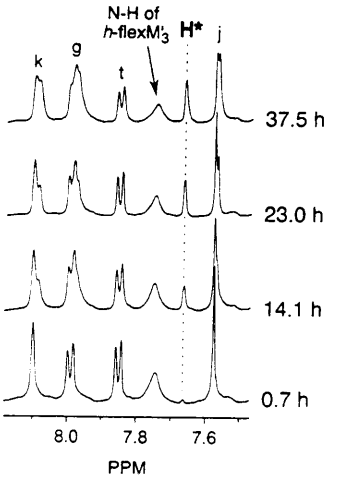

Figure 6. Examples of the ^{1}H NMR spectra at various times of the exchange reaction between *h*-flexM$_3$·hubCA$_3$ and *h*-flexM′$_3$ (500 MHz, $CDCl_3$). The resonance for H* marked by the dotted line shows the increase in concentration of *h*-flexM′$_3$·hubCA$_3$. This particular experiment was performed at 40 °C. The peak assignments correspond to the structure in Figure 1.

A. *h*-flexM$_3$ vs *h*-flexM′$_3$. The chemical structures of *h*-flexM$_3$ and *h*-flexM′$_3$ differ only by a single methyl group in each spoke, and we expected the stabilities of *h*-flexM$_3$·hubCA$_3$ and *h*-flexM′$_3$·hubCA$_3$ to be the same. Equilibrating a solution of 1:1 *h*-flexM$_3$·hubCA$_3$/free *h*-flexM′$_3$ led to an equimolar mixture of *h*-flexM$_3$·hubCA$_3$, *h*-flexM′$_3$·hubCA$_3$, free *h*-flexM$_3$, and free *h*-flexM′$_3$.

B. ^{1}H NMR Spectra of the Exchange Reaction. Figure 6 shows an example of the NMR spectra of the exchange reaction at various times. We monitored the appearance of the resonance at 7.66 ppm that corresponds to H* (Scheme I) of *h*-flexM′$_3$·hubCA$_3$. Comparison of the integral of this peak at various times during the exchange gave a measure of the progress of the reaction. We used the peak(s) at 8.09 ppm (labeled k in Figure 6) as a reference; these peaks correspond to NH protons of complexed hubCA$_3$. hubCA$_3$ is complexed with either *h*-flexM$_3$ or *h*-flexM′$_3$ throughout the course of the exchange reaction, and the chemical shift of the reference proton is slightly different in the two complexes. As the exchange reaction progresses, a shoulder appears on the peak at 8.09 ppm that corresponds to the reference proton in the *h*-flexM′$_3$·hubCA$_3$ complex. The important feature is that the *sum of the integrations* of the reference proton in *h*-flexM$_3$·hubCA$_3$ and *h*-flexM′$_3$·hubCA$_3$ does not change during the course of the reaction. Since the structures of *h*-flexM$_3$ and *h*-flexM′$_3$ are similar, most of the other resonances of *h*-flexM$_3$·hubCA$_3$ and *h*-flexM′$_3$·hubCA$_3$ (and free *h*-flexM$_3$ and free *h*-flexM′$_3$) overlap and thus cannot be used to monitor the exchange. During the exchange reaction, we do not observe any resonances that correspond to intermediates in the exchange process. The only resonances that we do observe correspond to *h*-flexM$_3$·hubCA$_3$, *h*-flexM′$_3$·hubCA$_3$, and free *h*-flexM$_3$ and *h*-flexM′$_3$. Data outlined above indicated that the initially formed *h*-flexM$_3$·hubCA$_3$ complex contains unsymmetrical species that isomerize to C_3-symmetrical *h*-flexM$_3$·hubCA$_3$. During the exchange reaction we do not detect resonances for these unsymmetrical species because the rate of isomerization of unsymmetrical to symmetrical species, although slow, it still substantially faster than the rate of the exchange reaction[11] and because the unsymmetrical species make up only a portion of the newly forming *h*-flexM′$_3$·hubCA$_3$.

(10) We have observed a similar hydrogen-bonded cyclic hexameric motif in the solid-state structure of the 1:1 complex between *N,N'*-bis (4-*tert*-butylphenyl)melamine and diethylbarbituric acid. Zerkowski, J. A.; Seto, C. T.; Whitesides, G. M. *J. Am. Chem. Soc.* **1992**, *114*, 5473.

(11) At room temperature, the exchange reaction progresses less than 5% toward completion (given an initial concentration of *h*-flexM$_3$·hubCA$_3$ of 5 mM) during the ~16 h that it takes for initially formed *h*-flexM$_3$·hubCA$_3$ to equilibrate to predominantly C_3-symmetrical isomers.

Scheme VI. Mechanism I[a]

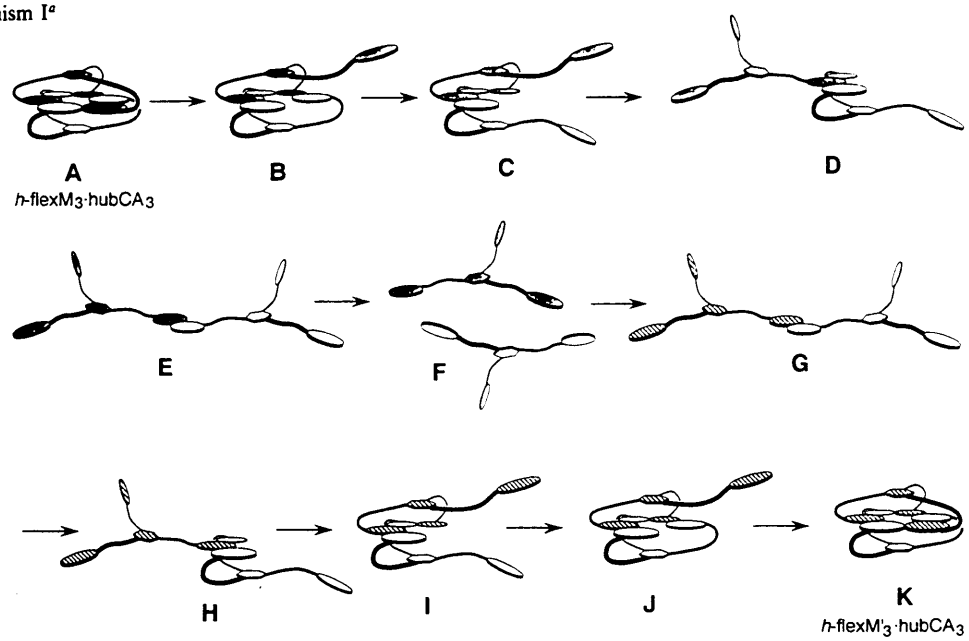

[a] Shaded circles correspond to *h*-flexM$_3$, striped circles correspond to *h*-flexM′$_3$, and unshaded circles correspond to hubCA$_3$.

C. Exchange at Different Concentrations. We monitored the rate of exchange between *h*-flexM$_3$·hubCA$_3$ and *h*-flexM′$_3$ at 22 °C in three reactions in which the relative initial concentrations of *h*-flexM$_3$·hubCA$_3$ and *h*-flexM′$_3$ were 1:1 (5.0:5.0 mM), 1:4 (5.0:20.0 mM), and 1:10 (2.5:25.0 mM) and analyzed the data according to eq 1.[12] We were not able to monitor the exchange reaction over a wider range of concentrations: at lower concentrations we were limited by poor signal-to-noise in the ^{1}H NMR spectra (using reasonable acquisition times) and at higher concentrations we were limited by the low solubility of the molecules in $CDCl_3$.

$$\left\{\frac{-[h\text{-flexM}'_3]_0}{[h\text{-flexM}_3\cdot h\text{ubCA}_3]_0 + [h\text{-flexM}'_3]_0}\right\} \ln\left\{1 - \frac{[h\text{-flexM}'_3\cdot h\text{ubCA}_3]_t}{[h\text{-flexM}'_3\cdot h\text{ubCA}_3]_\infty}\right\} = kt \quad (1)$$

Figure 7A gives a plot of the data and shows that the observed rate constant (the slope of the line) is independent of the concentration of free *h*-flexM′$_3$ over a factor of 10.[13] This result indicates that the exchange is unimolecular, the rate of the reaction in the forward direction depends only on [*h*-flexM$_3$·hubCA$_3$], and free *h*-flexM′$_3$ does not to participate in the rate-determining step for exchange.

D. Exchange at Different Temperatures. We also monitored the exchange reaction at four different temperatures (Figure 7B).[14] The inset graph in Figure 7B shows the rate constants plotted according to the Arrhenius equation.[15] From these data we can calculate that $\Delta H^\ddagger = 24 \pm 2$ kcal/mol, $\Delta S^\ddagger = -6 \pm 12$ eu ($T\Delta S^\ddagger = -2 \pm 4$ kcal/mol), and $\Delta G^\ddagger = 26 \pm 6$ kcal/mol (25 °C). The $\Delta S^\ddagger$ value has a large error because of the relatively small temperature range covered by these experiments. The fact that $\Delta S^\ddagger$ for this exchange reaction is close to zero is unexpected.

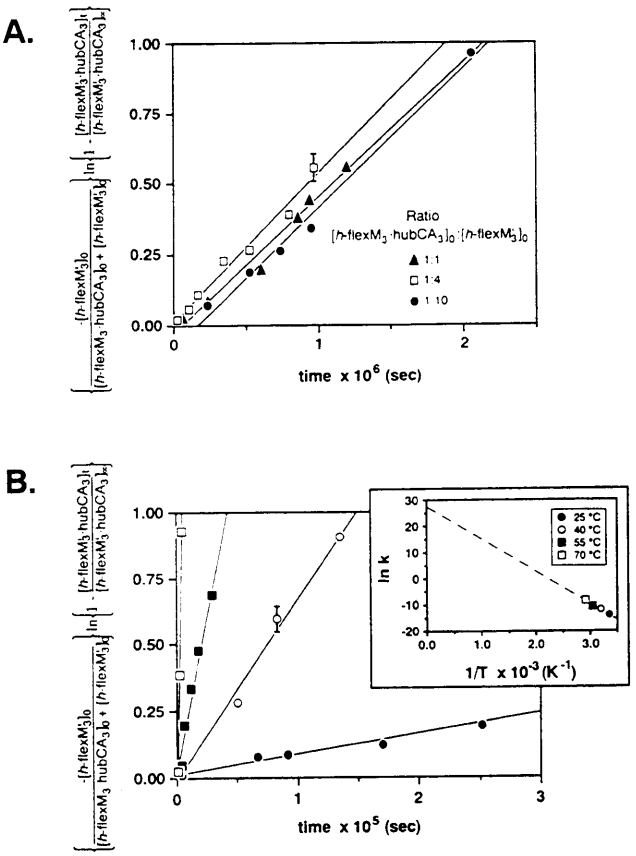

Figure 7. (A) Plot of the progress of the exchange reaction (Scheme I) as a function of time at three different ratios of [*h*-flexM$_3$·hubCA$_3$]$_0$:[*h*-flexM′$_3$]$_0$. The lines are derived from a least-squares analysis of the data. The slopes of the lines correspond to the rate constant k (s^{-1}). Representative error bars are shown and are based on an estimated ±5% uncertainty in determining the integration of peaks in the ^{1}H NMR spectra ($CDCl_3$). (B) Plot of the progress of the exchange reaction at four different temperatures. The inset is an Arrhenius plot of the data.

Discussion

Mechanism of the Exchange between *h*-flexM$_3$·hubCA$_3$ and *h*-flexM′$_3$. Our studies of the rate of exchange between *h*-flexM$_3$·hubCA$_3$ and *h*-flexM′$_3$ provide information relevant to the mechanism of this exchange reaction. First, the reaction is first-order in [*h*-flexM$_3$·hubCA$_3$] and zero-order in [*h*-flexM′$_3$].

(12) For the derivation of the general form of the kinetic equation associated with this type of exchange reaction, see: McKay, H. A. *J. Am. Chem. Soc.* **1943**, *65*, 702.

(13) The rate constants for these reactions are $k = 4.8 \times 10^{-7}$ (ratio [*h*-flexM$_3$·hubCA$_3$]$_0$:[*h*-flexM′$_3$]$_0$ = 1:1), 5.2×10^{-7} (ratio 1:4), and 5.0×10^{-7} s^{-1} (ratio 1:10).

(14) The rate constants for exchange at the four temperatures were $k = 7.7 \times 10^{-7}$ (25 °C), 6.8×10^{-6} (40 °C), 2.4×10^{-5} (55 °C), and 2.2×10^{-4} s^{-1} (70 °C).

(15) The *y*-intercept gives the pre-exponential factor ($A = 9.9 \times 10^{11}$ s^{-1}) and the slope gives E_a/R. The activation energy for the exchange between *h*-flexM$_3$·hubCA$_3$ and *h*-flexM′$_3$ is 25 kcal/mol.

Scheme VII. Mechanism II

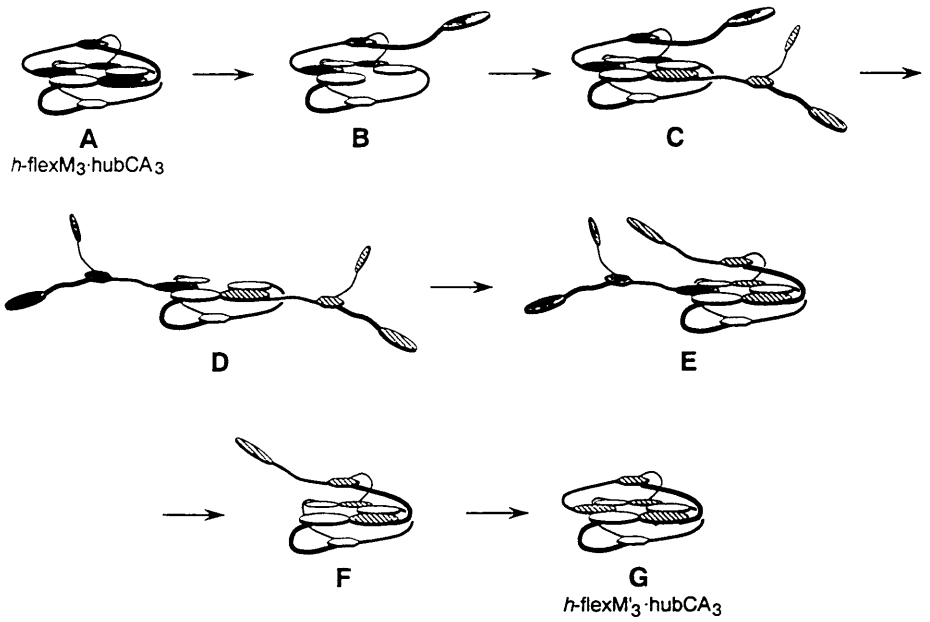

Table I. Values from the Literature for ΔH or ΔG of a Hydrogen Bond[a]

type of study	ΔH (kcal/mol)	ΔG (kcal/mol)
this study	1.3 ± 0.1 ($CHCl_3$)	
IR and NMR study of a cyclic intramolecular hydrogen bond in an α,ω-diamide[17]	1.4–1.6 (CH_2Cl_2)	
IR study of various *N*-butylacetamides[18]	1.4–2.6 ($CHCl_3$)	
calorimetric study of a modified G:C base pair[19]	1.9 ($CHCl_3$)	
average value from a number of literature sources, mostly of amide bonds in chloroform[20]		1.2 ± 0.2 ($CHCl_3$)
binding of peptides to vancomycin[21]		1.0–3.1 (H_2O)
stability studies on a number of RNase T1 mutants[22]		1.3 ± 0.6 (H_2O)
range of values from biological structures such as protein–ligand interactions and DNA base pairs[23]		0.5–1.8 (H_2O)

[a] The solvent is indicated in parentheses.

Second, we do not observe any intermediates during the exchange reaction. Third, $\Delta H^{\ddagger}$ is 24 kcal/mol and $\Delta S^{\ddagger}$ is close to zero. Here we consider two plausible mechanisms for the exchange reaction. These mechanisms are limiting cases, the operative mechanism may be a combination of the two extremes, and they are meant to span the range of possible mechanisms for this exchange reaction.

A. Mechanism I: Unimolecular Exchange. The first mechanism (Scheme VI) involves complete dissociation of *h*-flexM$_3$·hubCA$_3$, followed by complexation of free hubCA$_3$ with *h*-flexM′$_3$ to give *h*-flexM′$_3$·hubCA$_3$. This mechanism is consistent with our experimental data. Mechanism I predicts that the reaction should be first-order in [*h*-flexM$_3$·hubCA$_3$] and zero-order in [*h*-flexM′$_3$] and also yields a value for the average strength of a hydrogen bond that is consistent with literature precedent.

B. Mechanism II: Bimolecular Exchange. The second mechanism (Scheme VII) involves a first step in which one spoke of *h*-flexM$_3$ dissociates from the hydrogen-bonding network, breaking six hydrogen bonds, to give intermediate B. B is stabilized through hydrogen bonding with free *h*-flexM′$_3$. The remainder of the exchange takes place through breaking hydrogen bonds between *h*-flexM$_3$ and hubCA$_3$ and reforming these bonds with *h*-flexM′$_3$. If this mechanism were operative, we would expect the rate of reaction to be dependent on the concentrations of both *h*-flexM$_3$·hubCA$_3$ and *h*-flexM′$_3$. This expectation is contrary to our experimental observations.

Thermodynamic Considerations in the Exchange Mechanism. Scheme VIII shows energy level diagrams for mechanisms I and II.[16]

A. Mechanism I: Unimolecular Exchange. In mechanism I, intermediates B–F are not stabilized through hydrogen bonding with *h*-flexM′$_3$, and the rate of exchange should be zero-order in [*h*-flexM′$_3$], as was observed experimentally. The reaction is unimolecular and the rate of exchange is determined by the rate of dissociation of *h*-flexM$_3$·hubCA$_3$ into free components. The first step (A → B) has a small rate constant because six hydrogen bonds are broken. In the other steps leading to the transition state, only three hydrogen bonds are broken.

B. $\Delta H^{\ddagger}$. If mechanism I is operative, *h*-flexM$_3$ and hubCA$_3$ are fully dissociated in the transition state, and $\Delta H^{\ddagger}$ = 24 kcal/mol reflects the breaking of 18 hydrogen bonds. This mechanism gives

Scheme VIII. Reaction Coordinate Diagrams for Mechanisms I and II

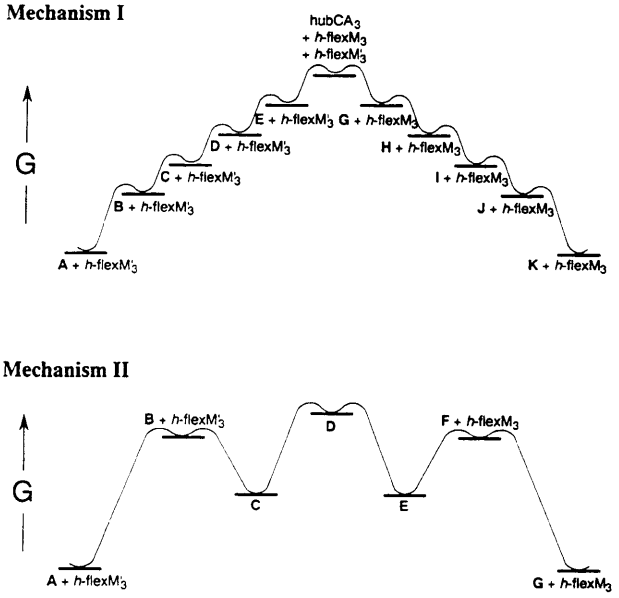

(16) In the energy level diagram for mechanism II, we do not have any information about the relative energies of intermediates B, D, and F. We also do not have any information about the energies of the transition states *between intermediates* in the exchange process (i.e., $\Delta G^{\ddagger}$ for B → A vs B → C).

Scheme VI. Mechanism I[a]

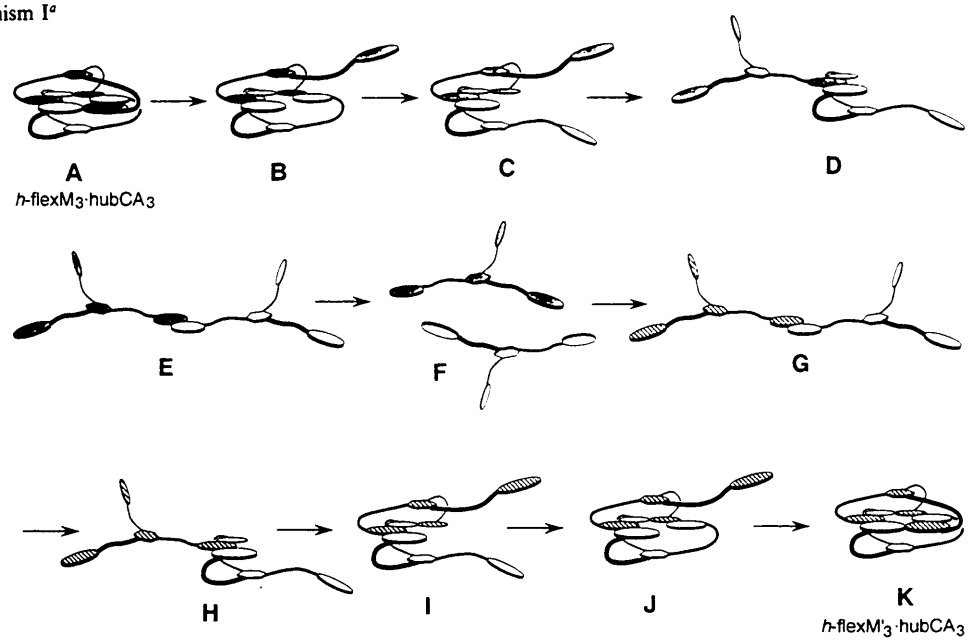

[a] Shaded circles correspond to *h*-flexM$_3$, striped circles correspond to *h*-flexM′$_3$, and unshaded circles correspond to hubCA$_3$.

C. Exchange at Different Concentrations. We monitored the rate of exchange between *h*-flexM$_3$·hubCA$_3$ and *h*-flexM′$_3$ at 22 °C in three reactions in which the relative initial concentrations of *h*-flexM$_3$·hubCA$_3$ and *h*-flexM′$_3$ were 1:1 (5.0:5.0 mM), 1:4 (5.0:20.0 mM), and 1:10 (2.5:25.0 mM) and analyzed the data according to eq 1.[12] We were not able to monitor the exchange reaction over a wider range of concentrations: at lower concentrations we were limited by poor signal-to-noise in the ^{1}H NMR spectra (using reasonable acquisition times) and at higher concentrations we were limited by the low solubility of the molecules in $CDCl_3$.

$$\left\{\frac{-[h\text{-flexM}'_3]_0}{[h\text{-flexM}_3\text{·hubCA}_3]_0 + [h\text{-flexM}'_3]_0}\right\} \ln\left\{1 - \frac{[h\text{-flexM}'_3\text{·hubCA}_3]_t}{[h\text{-flexM}'_3\text{·hubCA}_3]_\infty}\right\} = kt \quad (1)$$

Figure 7A gives a plot of the data and shows that the observed rate constant (the slope of the line) is independent of the concentration of free *h*-flexM′$_3$ over a factor of 10.[13] This result indicates that the exchange is unimolecular, the rate of the reaction in the forward direction depends only on [*h*-flexM$_3$·hubCA$_3$], and free *h*-flexM′$_3$ does not to participate in the rate-determining step for exchange.

D. Exchange at Different Temperatures. We also monitored the exchange reaction at four different temperatures (Figure 7B).[14] The inset graph in Figure 7B shows the rate constants plotted according to the Arrhenius equation.[15] From these data we can calculate that $\Delta H^\ddagger = 24 \pm 2$ kcal/mol, $\Delta S^\ddagger = -6 \pm 12$ eu ($T\Delta S^\ddagger = -2 \pm 4$ kcal/mol), and $\Delta G^\ddagger = 26 \pm 6$ kcal/mol (25 °C). The $\Delta S^\ddagger$ value has a large error because of the relatively small temperature range covered by these experiments. The fact that $\Delta S^\ddagger$ for this exchange reaction is close to zero is unexpected.

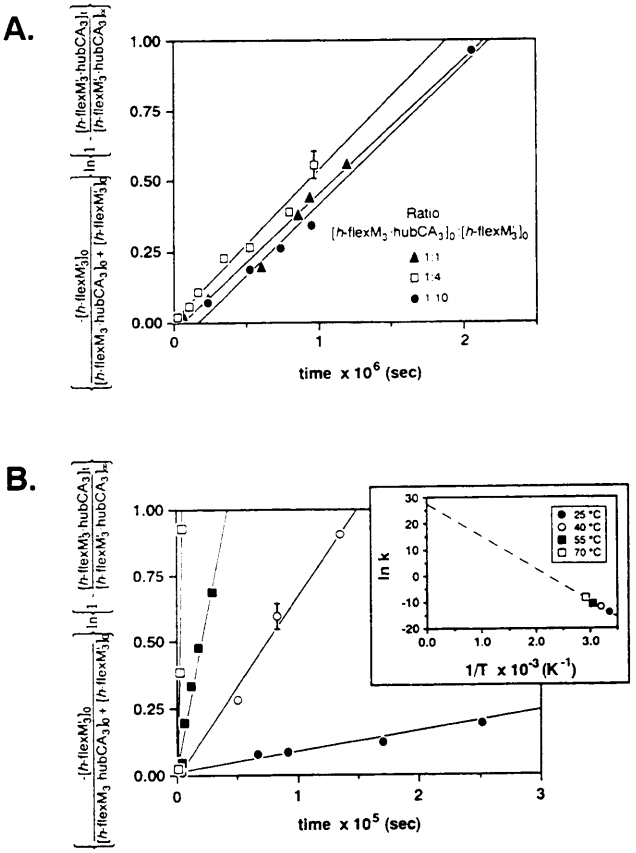

Figure 7. (A) Plot of the progress of the exchange reaction (Scheme I) as a function of time at three different ratios of [*h*-flexM$_3$·hubCA$_3$]$_0$:[*h*-flexM′$_3$]$_0$. The lines are derived from a least-squares analysis of the data. The slopes of the lines correspond to the rate constant k (s^{-1}). Representative error bars are shown and are based on an estimated ±5% uncertainty in determining the integration of peaks in the ^{1}H NMR spectra ($CDCl_3$). (B) Plot of the progress of the exchange reaction at four different temperatures. The inset is an Arrhenius plot of the data.

Discussion

Mechanism of the Exchange between *h*-flexM$_3$·hubCA$_3$ and *h*-flexM′$_3$. Our studies of the rate of exchange between *h*-flexM$_3$·hubCA$_3$ and *h*-flexM′$_3$ provide information relevant to the mechanism of this exchange reaction. First, the reaction is first-order in [*h*-flexM$_3$·hubCA$_3$] and zero-order in [*h*-flexM′$_3$].

(12) For the derivation of the general form of the kinetic equation associated with this type of exchange reaction, see: McKay, H. A. *J. Am. Chem. Soc.* **1943**, *65*, 702.

(13) The rate constants for these reactions are $k = 4.8 \times 10^{-7}$ (ratio [*h*-flexM$_3$·hubCA$_3$]$_0$:[*h*-flexM′$_3$]$_0$ = 1:1), 5.2×10^{-7} (ratio 1:4), and 5.0×10^{-7} s^{-1} (ratio 1:10).

(14) The rate constants for exchange at the four temperatures were $k = 7.7 \times 10^{-7}$ (25 °C), 6.8×10^{-6} (40 °C), 2.4×10^{-5} (55 °C), and 2.2×10^{-4} s^{-1} (70 °C).

(15) The *y*-intercept gives the pre-exponential factor ($A = 9.9 \times 10^{11}$ s^{-1}) and the slope gives E_a/R. The activation energy for the exchange between *h*-flexM$_3$·hubCA$_3$ and *h*-flexM′$_3$ is 25 kcal/mol.

Scheme VII. Mechanism II

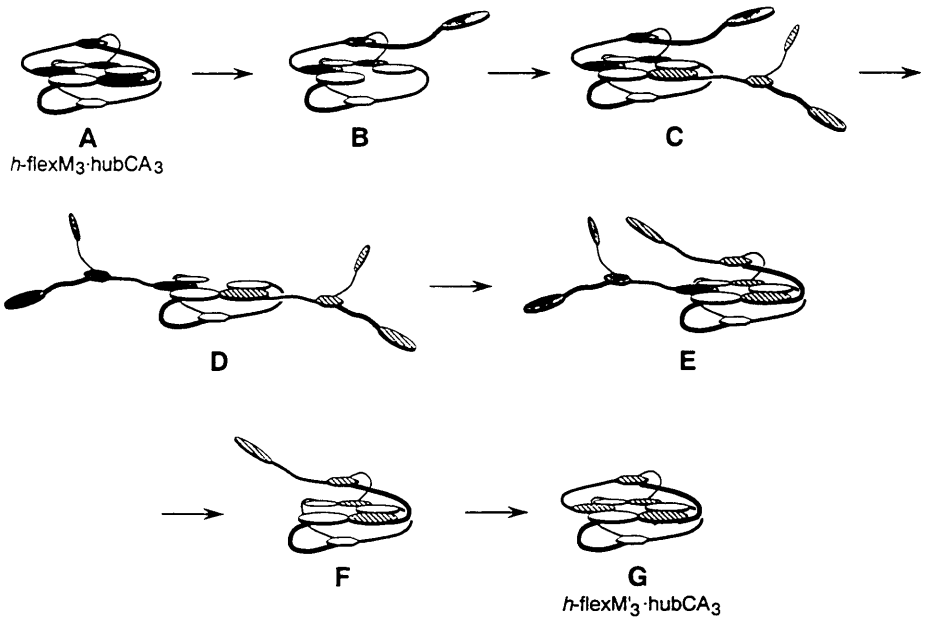

Table I. Values from the Literature for ΔH or ΔG of a Hydrogen Bond[a]

type of study	ΔH (kcal/mol)	ΔG (kcal/mol)
this study	1.3 ± 0.1 ($CHCl_3$)	
IR and NMR study of a cyclic intramolecular hydrogen bond in an α,ω-diamide[17]	1.4–1.6 (CH_2Cl_2)	
IR study of various *N*-butylacetamides[18]	1.4–2.6 ($CHCl_3$)	
calorimetric study of a modified G:C base pair[19]	1.9 ($CHCl_3$)	
average value from a number of literature sources, mostly of amide bonds in chloroform[20]		1.2 ± 0.2 ($CHCl_3$)
binding of peptides to vancomycin[21]		1.0–3.1 (H_2O)
stability studies on a number of RNase T1 mutants[22]		1.3 ± 0.6 (H_2O)
range of values from biological structures such as protein–ligand interactions and DNA base pairs[23]		0.5–1.8 (H_2O)

[a] The solvent is indicated in parentheses.

Second, we do not observe any intermediates during the exchange reaction. Third, $\Delta H^{\ddagger}$ is 24 kcal/mol and $\Delta S^{\ddagger}$ is close to zero. Here we consider two plausible mechanisms for the exchange reaction. These mechanisms are limiting cases, the operative mechanism may be a combination of the two extremes, and they are meant to span the range of possible mechanisms for this exchange reaction.

A. Mechanism I: Unimolecular Exchange. The first mechanism (Scheme VI) involves complete dissociation of *h*-flexM$_3$·hubCA$_3$, followed by complexation of free hubCA$_3$ with *h*-flexM′$_3$ to give *h*-flexM′$_3$·hubCA$_3$. This mechanism is consistent with our experimental data. Mechanism I predicts that the reaction should be first-order in [*h*-flexM$_3$·hubCA$_3$] and zero-order in [*h*-flexM′$_3$] and also yields a value for the average strength of a hydrogen bond that is consistent with literature precedent.

B. Mechanism II: Bimolecular Exchange. The second mechanism (Scheme VII) involves a first step in which one spoke of *h*-flexM$_3$ dissociates from the hydrogen-bonding network, breaking six hydrogen bonds, to give intermediate B. B is stabilized through hydrogen bonding with free *h*-flexM′$_3$. The remainder of the exchange takes place through breaking hydrogen bonds between *h*-flexM$_3$ and hubCA$_3$ and reforming these bonds with *h*-flexM′$_3$. If this mechanism were operative, we would expect the rate of reaction to be dependent on the concentrations of both *h*-flexM$_3$·hubCA$_3$ and *h*-flexM′$_3$. This expectation is contrary to our experimental observations.

Thermodynamic Considerations in the Exchange Mechanism. Scheme VIII shows energy level diagrams for mechanisms I and II.[16]

A. Mechanism I: Unimolecular Exchange. In mechanism I, intermediates B–F are not stabilized through hydrogen bonding with *h*-flexM′$_3$, and the rate of exchange should be zero-order in [*h*-flexM′$_3$], as was observed experimentally. The reaction is unimolecular and the rate of exchange is determined by the rate of dissociation of *h*-flexM$_3$·hubCA$_3$ into free components. The first step (A → B) has a small rate constant because six hydrogen bonds are broken. In the other steps leading to the transition state, only three hydrogen bonds are broken.

B. $\Delta H^{\ddagger}$. If mechanism I is operative, *h*-flexM$_3$ and hubCA$_3$ are fully dissociated in the transition state, and $\Delta H^{\ddagger}$ = 24 kcal/mol reflects the breaking of 18 hydrogen bonds. This mechanism gives

Scheme VIII. Reaction Coordinate Diagrams for Mechanisms I and II

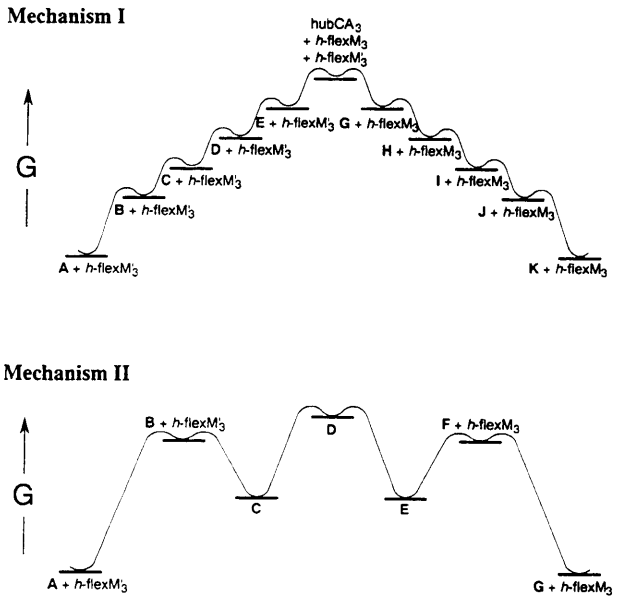

(16) In the energy level diagram for mechanism II, we do not have any information about the relative energies of intermediates B, D, and F. We also do not have any information about the energies of the transition states *between intermediates* in the exchange process (i.e., $\Delta G^{\ddagger}$ for B → A vs B → C).

an average enthalpy per hydrogen bond in *h*-flexM_3·hubCA_3 of 1.3 ± 0.1 kcal/mol (assuming that there is no other contribution to $\Delta H^{\ddagger}$ other than breaking hydroben bonds and that $\Delta H^{\ddagger} \approx \Delta H_0$ for formation of the complex from its constituent molecules). Table I shows several values from the literature of ΔH and ΔG of hydrogen bonds from a variety of systems; our value agrees with literature precedents.[17-23]

C. Entropy of Solvation. One possible way to rationalize the difference between the observed entropy for this process ($T\Delta S^{\ddagger} \approx 0$) and the value expected for dissociation of one, highly structured particle into two, relatively flexible ones is to attribute the difference to the entropy of solvation of free *h*-flexM_3 and free hubCA_3 in the transition state. In the transition state there are 18 sites available for hydrogen bonding with the solvent that were not available in the ground state.[24] To calculate the entropy of solvation of free *h*-flexM_3 and free hubCA_3, we hypothesize that the hydrogen-bonding sites on these molecules are similar to those on DMF and make use of IR and NMR data on the binding of DMF to chloroform. The association constant of DMF with chloroform is $K = 0.89$ L/mol, and the entropy of association is −4.0 eu.[25] From this binding constant, the starting concentration of *h*-flexM_3·hubCA_3 in our experiments (5.0 mM), and the concentration of chloroform (12.5 M), we calculate that an average of 16.6 out of the 18 available hydrogen-bonding sites in the fully dissociated transition state would be bound to chloroform molecules. With these values, we arrive at an estimate for $-T\Delta S^{\ddagger}_{\text{solvation}}$ of free *h*-flexM_3 and free hubCA_3 of $-16.6 \times (-4.0 \text{ eu}) \times 298 \text{ K} \approx +19.8$ kcal/mol. This estimate is not quantitatively meaningful for this system, but it does indicate that $-T\Delta S^{\ddagger}_{\text{solvation}}$ could be positive and large enough to significantly offset the expected large negative value for $-T\Delta S^{\ddagger}$ from translational and conformational entropies on dissociation of *h*-flexM_3·hubCA_3 into two independent molecules.

Our analysis of mechanism I shows that this mechanism is compatible with experimental observations. The reaction is first-order in [*h*-flexM_3·hubCA_3] and zero-order in [*h*-flexM'_3], a result expected on the basis of mechanism I. The value for the enthalpy of a hydrogen bond that is derived from this mechanism is in good agreement with literature precedents. The low value of $T\Delta S^{\ddagger}$ for the reaction can be rationalized on the basis of the formation of hydrogen bonds with $CHCl_3$. Mechanism II is not consistent with our experimental results. The mechanism predicts a second-order rate of reaction and results in an estimate for the enthalpy of a hydrogen bond that is too high.[26]

Although our experiments suggest that mechanism I is the operative one, we have clearly not proven this mechanism rigorously. One prediction that we can make if mechanism I is operative is that the hydrogen-bonding characteristics and polarity of the solvent will have a large influence on the rate of the exchange reaction. Since the transition state of mechanism I has fully dissociated species, the only stabilization of this transition state comes from hydrogen bonding with the solvent. A solvent that is a stronger hydrogen-bond donor or acceptor than chloroform will stabilize the transition state and result in a faster rate of exchange. Conversely, a weaker hydrogen-bonding solvent will raise the free energy of the transition state and result in a slower rate of exchange. For mechanism II, the solvent should have only a minor influence on the rate of exchange because the transition state is stabilized through hydrogen bonding with *h*-flexM_3 rather than with the solvent. We are currently examining the rate of this exchange reaction in different solvents.

(17) Gellman, S. H.; Dado, G. P.; Liang, G. B.; Adams, B. R. *J. Am. Chem. Soc.* **1991**, *113*, 1164.
(18) Nikolic, A. D.; Tarjani-Rozsa, M.; Perisic-Janjic, N. U.; Petrik, A.; Antonovic, D. G. *J. Mol. Struct.* **1990**, *219*, 245.
(19) Williams, L. D.; Chawla, B.; Shaw, B. R. *Biopolymers* **1987**, *26*, 591.
(20) Schneider, H. J.; Juneja, R. K.; Simova, S. *Chem. Ber.* **1989**, *122*, 1211. Schneider, H. J. *Angew. Chem., Int. Ed. Engl.* **1991**, *30*, 1417.
(21) Cox, J. P. L.; Nicholls, I. A.; Williams, D. H. *J. Chem. Soc., Chem. Commun.* **1991**, 1295. Williams, D. H. *Aldrichimica Acta* **1991**, *24*, 71. Williams, D. H.; et al. *J. Am. Chem. Soc.* **1991**, *113*, 7020. Doig, A. J.; Williams, D. H. *J. Am. Chem. Soc.* **1992**, *114*, 338. Williams, D. H. *Aldrichimica Acta* **1992**, *25*, 9.
(22) Shirley, B. A.; Stanssens, P.; Hahn, U.; Pace, C. N. *Biochemistry* **1992**, *31*, 725.
(23) Fersht, A. R. *Trends Biochem. Sci.* **1987**, *12*, 301.
(24) We assume that the solvent, chloroform, is only a hydrogen-bond donor.
(25) Shaw, Y. H.; Li, N. C. *Can. J. Chem.* **1970**, *48*, 2090. Joesten, M. D.; Schaad, L. J. *Hydrogen Bonding*; Marcel Dekker, Inc.: New York, 1974.
(26) In mechanism II, there are a total of six hydrogen bonds that are broken in the transition state. This mechanism predicts an average enthalpy per hydrogen bond in *h*-flexM_3·hubCA_3 of 4.0 kcal/mol.

Conclusions

Stability of the CA_3·M_3 Hexamer. Our studies of *h*-flexM_3·hubCA_3 suggest that the 18 hydrogen bonds in the CA_3·M_3 hexamer contribute ~24 kcal/mol to the enthalpy of formation of self-assembled aggregates based on this motif. *h*-flexM_3·hubCA_3 is the most stable hydrogen-bonded structure that we have synthesized. The large enthalpy of formation is only partially offset by the loss in translational entropy, because only two particles, rather than four or five particles as in previous structures, associate to form the aggregate.[1,2]

Molecular Weight of *h*-flexM_3·hubCA_3. VPO results depend both on concentration and on choice of molecular weight standard (Figures 4 and 5). Our VPO analysis of *h*-flexM_3·hubCA_3 leads to an estimate of the molecular weight of the complex in chloroform solution that is higher than the calculated value. We believe that this high molecular weight is caused by nonspecific self-association of the aggregate, possibly attributable to the octadecyl side chains, rather than to the formation of dimers or higher oligomers with stoichiometries such as (*h*-flexM_3·hubCA_3)$_2$. We cannot, at present, rationalize the results from VPO in detail, but note the major importance of nonidealities in this experimental technique. Other techniques are consistent with the proposed 1 + 1 structure. In particular, ^{1}H NMR spectroscopy shows that the three spokes of both components of the aggregate are in indistinguishable environments, a result that is compatible with the proposed C_3-symmetrical structure and that is not consistent with dimeric structures. We cannot detect the presence of dimers by ^{1}H NMR spectroscopy. If they are present, these dimers must account for less than ~5% of the material.

Thermodynamics of Exchange. The thermodynamic analysis of the exchange reaction between *h*-flexM_3·hubCA_3 and *h*-flexM'_3 suggests that the exchange occurs through dissociation of the aggregate. Since the transition state for the dissociative mechanism corresponds to the free components in solution, study of the exchange reaction provides information about the assembly of the aggregate from dissociated species. From this study we infer that the average enthalpy of a hydrogen bond in these systems is ~1.3 kcal/mol. This value is compatible with values from the literature for hydrogen-bond strengths; this compatibility provides an independent measure of support for our conclusions concerning mechanisms.

Our calculations suggest that $\Delta S_{\text{solvation}}$ may make a significant contribution to the free energy of formation of self-assembled aggregates. The enthalpy of solvation is already accounted for in our experimental value of $\Delta H^{\ddagger}$. This transition-state enthalpy is the *change* in enthalpy in going from associated species to free components; we do not know the *absolute* value of the enthalpy of the hydrogen bonds in the aggregate.

Experimental Section

General Methods. NOE experiments were performed with a Bruker AM 500 instrument. Elemental analyses were performed by Spang Microanalytical Laboratory. THF was distilled from sodium benzophenone ketyl. Methylene chloride and triethylamine were distilled from calcium hydride. Dimethylformamide was dried and stored over 4-Å molecular sieves. The compounds that have a triazine unit in their chemical structures show doubling of several resonances in their ^{1}H and ^{13}C NMR spectra due to slow exchange of conformers around the NHR triazine bonds.

***N*-Octadecyl-*N'*-(*tert*-butyloxycarbonyl)-1,3-diaminobenzene (2).** *N*-(*tert*-Butyloxycarbonyl)-1,3-diaminobenzene (4.00 g, 19.2 mmol),[1] octadecyl bromide (6.43 g, 19.3 mmol), diisopropylethylamine (3.23 g, 4.36 mL, 25.0 mmol), and 40 mL of DMF were combined and heated at 115 °C for 3 h under a nitrogen atmosphere. The mixture was cooled to room temperature, and the solvent was removed by rotary evaporation

at aspirator pressure. The residue was partitioned between 300 mL of toluene and 150 mL of water, and the organic layer was washed twice with 150-mL portions of water and 100 mL of brine and dried over $MgSO_4$. The solvent was removed by rotary evaporation at aspirator pressure. The crude material was purified by flash chromatography (eluted with 1:1 CH_2Cl_2/hexanes) to give 4.62 g (10.0 mmol, 52%) of the product as a white solid: ^{1}H NMR (500 MHz, $CDCl_3$) δ 7.03 (dd, J = 8.0, 8.1 Hz, 1 H), 6.83 (s, 1 H), 6.51 (dd, J = 1.2, 7.9 Hz, 1 H), 6.47 (s, 1 H), 6.27 (dd, J = 1.7, 8.0 Hz, 1 H), 3.06 (t, J = 7.1 Hz, 2 H), 1.57 (m, 2 H), 1.50 (s, 9 H), 1.35 (m, 2 H), 1.26 (m, 28 H), 0.88 (t, J = 6.9 Hz, 3 H); ^{13}C NMR (125 MHz, $CDCl_3$) δ 152.67, 149.25, 139.39, 129.50, 107.56, 107.46, 103.02, 80.09, 44.04, 31.88, 29.64, 29.56, 29.41, 29.30, 28.34, 27.12, 22.62, 14.00; HRMS-FAB (M^+) calcd for $C_{29}H_{52}N_2O_5$ 460.4029, found 460.4039.

Methyl 2-Phthalimido-5-hydroxybenzoate (4). Methyl 5-hydroxyanthranilate **3** (4.52 g, 27.0 mmol)[27] and diisopropylethylamine (7.69 g, 10.36 mL, 59.5 mmol) were dissolved in 150 mL of THF and cooled in an ice bath under a nitrogen atmosphere. Phthaloyl dichloride (5.49 g, 3.90 mL, 27.0 mmol) was added dropwise to the solution, and the mixture was stirred at 0 °C for 1 h. The solvent was removed by rotary evaporation at aspirator pressure, and the residue was partitioned between 400 mL of ethyl acetate and 300 mL of 1 N aqueous HCl solution. The organic layer was washed with 300 mL of 1 N aqueous HCl solution, three times with 300-mL portions of water, and 100 mL of brine and dried over $MgSO_4$, and the solvent was removed by rotary evaporation at aspirator pressure. The crude material was purified by flash chromatography (eluted with 1:1 ethyl acetate/hexanes) to give 4.96 g (16.7 mmol, 62%) of the product as a white solid: ^{1}H NMR (300 MHz, DMSO-d_6) δ 10.30 (br s, 1 H), 7.95 (m, 4 H), 7.45 (d, J = 2.7 Hz, 1 H), 7.37 (d, J = 8.4 Hz, 1 H), 7.16 (dd, J = 2.7, 8.7 Hz, 1 H), 3.64 (s, 3 H); ^{13}C NMR (125 MHz, DMSO-d_6) δ 167.22, 164.59, 157.73, 134.55, 131.93, 131.55, 128.54, 123.23, 122.37, 119.89, 117.09, 52.07; HRMS-FAB (M^+) calcd for $C_{16}H_{11}NO_5$ 297.0637, found 297.0641.

Methyl 2-Phthalimido-5-(octadecyloxy)benzoate (5). Methyl 2-phthalimido-5-hydroxybenzoate (**4**) (4.96 g, 16.7 mmol), octadecyl bromide (8.35 g, 25.0 mmol), potassium carbonate (3.46 g, 25.0 mmol), and 18-crown-6 (2.21 g, 8.35 mmol) were combined with 50 mL of DMF, and the solution was heated at 80 °C for 2 h under a nitrogen atmosphere. The solution was cooled, and the solvent was removed by rotary evaporation at aspirator pressure. The residue was partitioned between 400 mL of ethyl acetate and 400 mL of water, and the aqueous layer was washed twice with 400-mL portions of water and 100 mL of brine and dried over $MgSO_4$. The solvent was removed by rotary evaporation at aspirator pressure. The crude material was purified by flash chromatography (eluted with 2:8 ethyl acetate/hexanes) to give 8.20 g (14.9 mmol, 89%) of the product as a white solid: ^{1}H NMR (400 MHz, $CDCl_3$) δ 7.95 (m, 2 H), 7.78 (m, 2 H), 7.65 (d, J = 2.9 Hz, 1 H), 7.28 (d, J = 8.8 Hz, 1 H), 7.18 (dd, J = 2.9, 8.6 Hz, 1 H), 4.03 (t, J = 6.5 Hz, 2 H), 3.72 (s, 3 H), 1.81 (m, 2 H), 1.47 (m, 2 H), 1.26 (m, 28 H), 0.88 (t, J = 6.8 Hz, 3 H); ^{13}C NMR (100 MHz, DMSO-d_6) δ 166.97, 164.34, 158.63, 134.20, 131.51, 131.48, 128.48, 123.50, 123.11, 118.65, 116.22, 67.98, 51.95, 31.24, 29.00, 28.96, 28.71, 28.67, 28.46, 25.35, 22.03, 13.74; HRMS-FAB (M^+) calcd for $C_{34}H_{47}NO_5$ 549.3454, found 549.3470.

Phthalimide 6. Methyl ester **5** (3.30 g, 6.0 mmol) was dissolved in 200 mL of THF, and to the solution were added 125 mL of water and 30 mL of 1 N aqueous NaOH solution. The mixture was stirred for 1 h at room temperature, and the THF was removed by rotary evaporation at aspirator pressure. The remaining material was partitioned between 300 mL of ethyl acetate and 150 mL of 1 N aqueous HCl solution. The organic layer was washed twice with 150-mL portions of water and 100 mL of brine and dried over $MgSO_4$, and the solvent was removed by rotary evaporation at aspirator pressure. The crude carboxylic acid was combined with 10 mL of thionyl chloride, and the solution was heated at reflux for 1 h under a nitrogen atmosphere. The reaction was diluted with 100 mL of toluene, and the solvent containing excess thionyl chloride was removed by rotary evaporation at aspirator pressure. The crude acid chloride was dried briefly at 0.1 Torr and then dissolved in 100 mL of CH_2Cl_2. The solution was cooled in an ice bath, and 1.82 g (2.51 mL, 18 mmol) of triethylamine was added followed by 2.30 g (5.0 mmol) of *N*-octadecyl-*N'*-(*tert*-butyloxycarbonyl)-1,3-diaminobenzene (**2**). The mixture was stirred for 1 h at room temperature, and the solvent was removed by rotary evaporation at aspirator pressure. The residue was partitioned between 400 mL of ethyl acetate and 300 mL of water, and the organic layer was washed twice with 300-mL portions of water and 100 mL of brine and dried over $MgSO_4$. The solvent was removed by rotary evaporation at aspirator pressure. The crude material was purified by flash chromatography (eluted with 15:85 ethyl acetate/hexanes) to give 4.43 g (4.53 mmol, 91% based on amine **2**) as a waxy solid: ^{1}H NMR (300 MHz, $CDCl_3$) δ 7.93 (m, 2 H), 7.77 (m, 2 H), 7.28 (m, 2 H), 7.17 (m, 2 H), 7.01 (d, J = 7.7 Hz, 1 H), 6.88 (d, J = 7.6 Hz, 1 H), 6.64 (s, 1 H), 6.47 (s, 1 H), 4.11 (t, J = 7.1 Hz, 2 H), 3.65 (m, 2 H), 1.63 (m, 2 H), 1.50 (m, 11 H), 1.26 (m, 60 H), 0.88 (m, 6 H); ^{13}C NMR (125 MHz, DMSO-d_6) δ 166.67, 152.30, 140.16, 134.08, 131.47, 130.34, 128.34, 122.89, 116.42, 78.67, 67.75, 31.08, 28.83, 28.80, 28.63, 28.48, 28.16, 27.86, 25.82, 25.09, 21.84, 13.54; HRMS-FAB (M + H^+) calcd for $C_{62}H_{96}N_3O_6$ 978.7299, found 978.7311.

Amine 7. Phthalimide **6** (4.25 g, 4.34 mmol) and hydrazine (1 mL) were dissolved in 75 mL of methanol, and the solution was heated at reflux for 1 h under a nitrogen atmosphere. The mixture was cooled and the solvent was removed by rotary evaporation at aspirator pressure. The residue was partitioned between 350 mL of ethyl acetate and 350 mL of water, and the organic layer was washed twice with 300-mL portions of water and 100 mL of brine and dried over $MgSO_4$. The solvent was removed by rotary evaporation at aspirator pressure. The crude material was used in the subsequent reaction without further purification: ^{1}H NMR (500 MHz, 1:1 $CDCl_3$/DMSO-d_6) δ 9.28 (s, 1 H), 7.44 (s, 1 H), 7.23 (d, J = 7.6 Hz, 1 H), 7.03 (t, J = 8.0 Hz, 1 H), 6.56 (m, 3 H), 6.33 (d, J = 2.2 Hz, 1 H), 5.15 (br s, 2 H), 3.74 (t, J = 7.3 Hz, 2 H), 3.49 (t, J = 6.4 Hz, 2 H), 1.47 (m, 13 H), 1.24 (m, 60 H), 0.86 (m, 6 H); ^{13}C NMR (125 MHz, 1:1 $CDCl_3$/DMSO-d_6) δ 169.17, 152.32, 148.80, 143.31, 140.33, 140.16, 128.41, 120.76, 119.98, 118.21, 117.02, 116.37, 115.95, 113.85, 67.91, 49.04, 31.14, 28.89, 28.57, 27.89, 27.16, 26.15, 25.21, 21.92, 13.65; HRMS-FAB (M^+) calcd for $C_{54}H_{93}N_3O_4$ 847.7166, found 847.7181.

Biuret 8. Crude amine **7** (3.52 g, 4.15 mmol) from the previous reaction was dissolved in 300 mL of DMF and 50 mL of water, and the solution was heated to 95 °C in an oil bath. To the solution was added 5.0 g of K_2HPO_4 and 5.0 g (33.8 mmol) of nitrobiuret and the mixture was stirred for 15 min. The addition of K_2HPO_4 (5.0 g) and nitrobiuret (5.0 g)[1] was repeated two more times at 15-min intervals. The reaction was cooled to room temperature, and the solvents were removed by rotary evaporation at aspirator pressure. The residue was partitioned between 400 mL of ethyl acetate and 300 mL of 1 N aqueous HCl solution. The organic layer was washed three times with 300-mL portions of water and 100 mL of brine and dried over $MgSO_4$, and the solvent was removed by rotary evaporation at aspirator pressure. The crude material was purified by flash chromatography (eluted with 4:6 ethyl acetate/hexanes) to give 3.32 g (3.55 mmol, 86%) of the product as a white solid: ^{1}H NMR (500 MHz, 1:1 $CDCl_3$/DMSO-d_6) δ 9.92 (br s, 1 H), 9.14 (s, 1 H), 9.03 (s, 2 H), 7.65 (br s, 1 H), 7.46 (br s, 1 H), 7.18 (br s, 1 H), 7.00 (br s, 1 H), 6.65 (br m, 4 H), 4.05 (br s, 2 H), 3.75 (br s, 2 H), 1.57 (m, 4 H), 1.49 (s, 9 H), 1.25 (m, 60 H), 0.87 (m, 6 H); ^{13}C NMR (100 MHz, 1:1 $CDCl_3$/DMSO-d_6) δ 167.36, 155.55, 152.63, 152.30, 139.96, 128.38, 120.65, 117.09, 116.41, 115.56, 112.66, 67.52, 31.22, 28.99, 28.65, 27.94, 26.93, 26.27, 25.32, 22.01, 13.72; HRMS-FAB (M + Na^+) calcd for $C_{56}H_{95}N_5O_6Na$ 956.7180, found 956.7175.

Isocyanurate 9. Biuret **8** (3.29 g, 3.52 mmol) and 1,1'-carbonyldiimidazole (2.28 g, 14.1 mmol) were dissolved in 80 mL of dry THF, and the solution was cooled in an ice bath under a nitrogen atmosphere. To the mixture was added 21.1 mL of a 1 N solution of potassium *tert*-butoxide in THF, and the reaction was stirred for 15 min at 0 °C and at room temperature for 4 h. The solvent was removed by rotary evaporation at aspirator pressure, and the residue was partitioned between 350 mL of ethyl acetate and 500 mL of 0.1 N aqueous HCl solution. The organic layer was washed twice with 300-mL portions of water and 100 mL of brine and dried over $MgSO_4$, and the solvent was removed by rotary evaporation at aspirator pressure. The crude material was purified by flash chromatography (eluted with 1:2 ethyl acetate/hexanes) to give 2.35 g (2.45 mmol, 70%) of the product as a white solid: ^{1}H NMR (500 MHz, 1:1 $CDCl_3$/DMSO-d_6) δ 11.58 (s, 2 H), 9.30 (s, 1 H), 7.65 (br s, 1 H), 7.23 (m, 2 H), 6.96 (br s, 1 H), 6.84 (br s, 2 H), 6.49 (br s, 1 H), 3.73 (br s, 2 H), 3.54 (br s, 2 H), 1.50 (m, 13 H), 1.24 (m, 60 H), 0.86 (m, 6 H); ^{13}C NMR (100 MHz, 1:1 $CDCl_3$/DMSO-d_6) δ 165.08, 157.08, 149.51, 148.63, 143.23, 140.33, 133.67, 131.47, 128.60, 122.01, 116.57, 115.75, 114.41, 67.71, 49.31, 31.28, 29.04, 28.21, 28.00, 26.87, 26.11, 25.20, 22.06, 13.80; HRMS-FAB (M + Na^+) calcd for $C_{57}H_{93}N_5O_7Na$ 982.6972, found 982.6992.

Amino Isocyanurate 10. Cyanurate **9** (2.30 g, 2.39 mmol) was dissolved in 75 mL of CH_2Cl_2 and the solution was cooled in an ice bath. Trifluoroacetic acid (10 mL) was added to the solution and the mixture was stirred at room temperature for 2 h. The solvent containing trifluoroacetic acid was removed by rotary evaporation at aspirator pressure, and the residue was partitioned between 350 mL of ethyl acetate and 300 mL of 1:1 saturated aqueous $NaHCO_3$ solution/water. The organic layer was washed twice with 300-mL portions of water and 100 mL of brine and dried over $MgSO_4$, and the solvent was removed by rotary evapo-

(27) Van der Stelt, C.; Suurmond, B. G.; Nauta, W. T. *Recl. Trav. Chim. Pays-Bas* **1953**, *72*, 195.

ration at aspirator pressure. The crude material was purified by flash chromatography (eluted with 4:6 ethyl acetate/hexanes) to give 1.79 g (2.08 mmol, 87%) of the product as a white foam: ^{1}H NMR (400 MHz, 1:9 $CDCl_3$/DMSO-d_6) δ 11.59 (s, 2 H), 7.18 (br s, 1 H), 6.83 (br s, 2 H), 6.60 (br s, 1 H), 6.54 (br s, 1 H), 6.47 (br s, 1 H), 6.41 (br s, 1 H), 5.24 (br s, 2 H), 3.68 (br s, 2 H), 3.61 (br s, 2 H), 1.54 (br s, 2 H), 1.43 (br s, 2 H), 1.24 (m, 60 H), 0.86 (m, 6 H); ^{13}C NMR (100 MHz, 1:9 $CDCl_3$/DMSO-d_6) δ 164.75, 157.04, 149.45, 148.54, 147.67, 143.59, 133.79, 131.08, 128.93, 125.33, 116.17, 115.85, 114.55, 112.93, 67.66, 49.56, 31.24, 28.96, 28.66, 28.27, 26.82, 26.19, 25.27, 22.02, 13.72; HRMS-FAB (M + Na^+) calcd for $C_{52}H_{85}N_5O_5Na$ 882.6448, found 882.6450.

hubCA$_3$. Amino cyanurate **10** (1.44 g, 1.67 mmol) and diisopropylethylamine (0.26 g, 0.35 mL, 2.0 mmol) were dissolved in 50 mL of CH_2Cl_2, and the solution was cooled in an ice bath under a nitrogen atmosphere. To the solution was added 148 mg (0.56 mmol) of 1,3,5-benzenetricarboxylic acid chloride and the mixture was stirred for 1 h at 0 °C. The reaction mixture was poured into 250 mL of ethyl acetate and 150 mL of 0.1 N aqueous HCl solution. The organic layer was washed twice with 250-mL portions of water and 100 mL of brine and dried over $MgSO_4$, and the solvents were removed by rotary evaporation at aspirator pressure. The crude material was purified by flash chromatography (eluted with 3:97 methanol/CH_2Cl_2) to give 1.38 g (0.50 mmol, 91%) of the product as a white solid: ^{1}H NMR (400 MHz, 1:1 $CDCl_3$/DMSO-d_6) δ 11.63 (s, 6 H), 10.67 (s, 3 H), 8.90 (s, 3 H), 8.16 (br s, 3 H), 7.69 (br s, 3 H), 7.18 (br s, 3 H), 7.06 (br m, 6 H), 6.85 (br s, 3 H), 6.56 (br s, 3 H), 3.89 (br s, 6 H), 3.83 (br s, 6 H), 1.54 (br s, 12 H), 1.22 (br m, 180 H), 0.85 (m, 18 H); ^{13}C NMR (100 MHz, 1:1 $CDCl_3$/DMSO-d_6) δ 165.00, 164.07, 157.05, 149.47, 148.56, 143.00, 139.66, 134.84, 131.25, 129.82, 128.59, 125.33, 123.89, 118.64, 116.30, 114.75, 67.83, 49.77, 31.23, 29.01, 28.65, 28.28, 26.18, 25.24, 22.01, 13.72. Anal. Calcd for $C_{165}H_{255}N_{15}O_{18}$: C, 72.41; H, 9.39; N, 7.68. Found: C, 72.50; H, 9.42; N, 7.72.

4-Hydroxybutyl 2-Aminobenzoate (11). A 500-mL round-bottomed flask equipped with a Dean–Stark trap and a stirring bar was charged with 6.86 g (50 mmol) of anthranilic acid, 45.1 g (44.3 mL, 500 mmol) of 1,4-butanediol, 3.8 g (20 mmol) of *p*-toluenesulfonic acid, and 200 mL of toluene, and the mixture was heated at reflux for 36 h. Approximately 5 mL of water was collected in the trap. The mixture was cooled and poured into 200 mL of ethyl acetate and 300 mL of 1:2 saturated aqueous $NaHCO_3$ solution/water. The organic layer was washed three times with 300-mL portions of 2:1 water/saturated aqueous Na_2CO_3 solution, three times with 400-mL portions of water, and 200 mL of brine and dried over $MgSO_4$, and the solvents were removed by rotary evaporation at aspirator pressure. The crude material was purified by flash chromatography (eluted with 1:1 ethyl acetate/hexanes) to give 3.20 g (15.3 mmol, 31%) of the product as a yellow oil: ^{1}H NMR (400 MHz, DMSO-d_6) δ 7.71 (d, J = 7.9 Hz, 1 H), 7.25 (m, 1 H), 6.77 (d, J = 8.3 Hz, 1 H), 6.65 (s, 2 H), 6.53 (m, 1 H), 4.48 (t, J = 5.4 Hz, 1 H), 4.21 (t, J = 6.5 Hz, 2 H), 4.45 (m, 2 H), 1.72 (m, 2 H), 1.54 (m, 2 H); ^{13}C NMR (100 MHz, $CDCl_3$) δ 168.00, 150.29, 133.86, 130.90, 116.53, 115.98, 110.53, 63.93, 61.82, 28.91, 24.95; HRMS-FAB (M^+) calcd for $C_{11}H_{15}NO_3$ 209.1052, found 209.1041.

2-[[4-Amino-6-[(3,3-dimethylbutyl)amino]-1,3,5-triazin-2-yl]amino]-benzoic Acid 4-Hydroxybutyl Ester (12). A 250-mL round-bottomed flask equipped with a stirring bar was charged with 2.71 g (12.9 mmol) of amine **11**, 1.84 g (2.48 mL, 14.2 mmol) of diisopropylethylamine, and 60 mL of THF. The solution was cooled in an ice bath under a nitrogen atmosphere, and 2.62 g (14.2 mmol) of cyanuric chloride was added in one portion. The solution was stirred in the ice bath for 1 h, and then gaseous ammonia was passed over the solution in a gentle stream for an additional 1 h. The solution was warmed to room temperature and the solvent was removed by rotary evaporation at aspirator pressure. The residue was taken up in 250 mL of ethyl acetate, washed four times with 200-mL portions of water and once with 100 mL of brine, and dried over $MgSO_4$. The solvent was removed by rotary evaporation at aspirator pressure, giving the intermediate chlorotriazine as a white solid. This crude chlorotriazine was combined with 2.53 g (3.36 mL, 25.0 mmol) of neohexylamine, 3.23 g (4.36 mL, 25.0 mmol) of diisopropylethylamine, and 100 mL of THF. The solution was heated at reflux for 5 h under a nitrogen atmosphere and cooled to room temperature, and the solvent was removed by rotary evaporation at aspirator pressure. The residue was taken up in 400 mL of ethyl acetate, washed four times with 300-mL portions of water and once with 150 mL of brine, and dried over $MgSO_4$, and the solvent was removed by rotary evaporation at aspirator pressure. The product was purified by flash chromatography (eluted with ethyl acetate) to give 4.09 g (10.17 mmol, 88%) of the product as a white solid: ^{1}H NMR (400 MHz, DMSO-d_6) δ 10.31, 10.26 (two conformers, s, 1 H), 9.01, 8.96 (two conformers, d, J = 8.6 Hz, 1 H), 7.96 (m, 1 H), 7.50 (m, 1 H), 7.00 (m, 2 H), 6.63 (s, 1 H), 6.47 (s, 1 H), 4.49 (t, J = 5.1 Hz, 1 H), 4.30 (t, J = 6.4 Hz, 2 H), 3.46 (m, 2 H), 3.28 (m, 2 H), 1.76, (m, 2 H), 1.56 (m, 2 H), 1.44 (m, 2 H), 0.93 (s, 9 H); ^{13}C NMR (100 MHz, DMSO-d_6) δ 167.64, 167.10, 166.74, 166.00, 165.80, 164.34, 164.00, 143.12, 142.96, 134.03, 133.78, 130.67, 120.17, 119.98, 113.98, 113.65, 64.95, 60.34, 43.17, 42.68, 36.61, 29.52, 29.34, 29.02, 24.97; HRMS-FAB (M + H^+) calcd for $C_{20}H_{31}N_6O_3$ 403.2457, found 403.2458.

***h*-flexM$_3$.** A 100-mL round-bottomed flask equipped with a stirring bar was charged with 1.81 g (4.5 mmol) of alcohol **12**, 0.65 g (0.87 mL, 5.0 mmol) of diisopropylethylamine, and 40 mL of THF. The solution was cooled in an ice bath under a nitrogen atmosphere, 0.40 g (1.5 mmol) of 1,3,5-benzenetricarboxylic acid chloride was added, and the solution was stirred at 0 °C for 2 h and at room temperature for 12 h. The solvent was removed by rotary evaporation at aspirator pressure, and the residue was taken up in 300 mL of ethyl acetate. The organic layer was washed twice with 150-mL portions of water, twice with 100-mL portions of saturated aqueous sodium carbonate solution, twice with 150-mL portions of water, and once with 100 mL of brine and dried over $MgSO_4$, and the solvent was removed by rotary evaporation at aspirator pressure. The crude product was purified by flash chromatography (eluted with ethyl acetate followed by 97:3 ethyl acetate/methanol) to give 1.77 g (1.29 mmol, 86%) of the product as a white foam: ^{1}H NMR (400 MHz, DMSO-d_6) δ 10.27, 10.21 (two conformers, s, 3 H), 8.96, 8.89 (two conformers, d, J = 8.5 Hz, 3 H), 8.54 (s, 3 H), 7.91 (dd, J = 1.1, 7.9 Hz, 3 H), 7.48, 7.40 (two conformers, t, J = 7.7 Hz, 3 H), 6.94 (m, 6 H), 6.61 (s, 3 H), 6.44 (s, 3 H), 4.37 (m, 12 H), 3.25 (m, 6 H), 1.89 (m, 12 H), 1.42 (m, 6 H), 0.91 (s, 27 H); ^{13}C NMR (100 MHz, DMSO-d_6) δ 167.47, 167.04, 166.67, 165.92, 165.73, 164.21, 163.90, 143.09, 142.94, 133.94, 133.66, 133.27, 130.75, 130.52, 119.93, 119.81, 113.61, 113.38, 65.03, 64.46, 43.10, 42.63, 36.53, 29.25, 24.88, 24.78; HRMS-FAB (M + H^+) calcd 1363.7063, found 1363.7014. Anal. Calcd for $C_{69}H_{90}N_{18}O_{12}$: C, 60.78; H, 6.65; N, 18.49. Found: C, 60.73; H, 6.68; N, 18.40.

4-Hydroxybutyl 2-Amino-5-methylbenzoate (13). A 1-L round-bottomed flask equipped with a Dean–Stark trap and a stirring bar was charged with 12.5 g (82.7 mmol) of 5-methylanthranilic acid, 74.5 g (73.3 mL, 827 mmol) of 1,4-butanediol, 15.9 g (10.7 mL, 165 mmol) of methanesulfonic acid, and 400 mL of toluene, and the mixture was heated at reflux for 24 h. The mixture was cooled and poured into 400 mL of ethyl acetate and 600 mL of 1:2 saturated aqueous $NaHCO_3$ solution/water. The organic layer was washed three times with 500-mL portions of 2:1 water/saturated aqueous Na_2CO_3 solution, three times with 400-mL portions of water, and 200 mL of brine and dried over $MgSO_4$, and the solvents were removed by rotary evaporation at aspirator pressure. The crude material was purified by flash chromatography (eluted with 1:1 ethyl acetate/hexanes) to give 4.15 g (18.6 mmol, 23%) of the product as a tan solid: ^{1}H NMR (400 MHz, $CDCl_3$) δ 7.63 (d, J = 1.2 Hz, 1 H), 7.06 (dd, J = 2.0, 8.3 Hz, 1 H), 6.57 (d, J = 8.3 Hz, 1 H), 4.68 (br s, 3 H), 4.27 (t, J = 6.5 Hz, 2 H), 3.66 (t, J = 6.5 Hz, 2 H), 2.21 (s, 3 H), 1.82 (m, 2 H), 1.68 (m, 2 H); ^{13}C NMR (100 MHz, $CDCl_3$) δ 168.01, 148.00, 134.99, 130.46, 125.17, 116.76, 110.56, 63.91, 61.85, 28.92, 25.00, 20.04; HRMS-FAB (M^+) calcd for $C_{12}H_{17}NO_3$ 223.1208, found 223.1210.

2-[[4-Amino-6-[(3,3-dimethylbutyl)amino]-1,3,5-triazin-2-yl]amino]-5-methylbenzoic Acid 4-Hydroxybutyl Ester (14). A 250-mL round-bottomed flask equipped with a stirring bar was charged with 2.65 g (11.9 mmol) of amine **13**, 2.15 g (2.90 mL, 16.6 mmol) of diisopropylethylamine, and 75 mL of THF. The solution was cooled in an ice bath under a nitrogen atmosphere, and 2.85 g (15.4 mmol) of cyanuric chloride was added in one portion. The solution was stirred in the ice bath for 1 h, and then gaseous ammonia was passed over the solution in a gentle stream for an additional 1 h. The solution was warmed to room temperature and the solvent was removed by rotary evaporation at aspirator pressure. The residue was taken up in 300 mL of ethyl acetate, washed four times with 200-mL portions of water and once with 100 mL of brine, and dried over $MgSO_4$. The solvent was removed by rotary evaporation at aspirator pressure, giving the intermediate chlorotriazine as a white solid. This crude chlorotriazine was combined with 2.53 g (3.36 mL, 25.0 mmol) of neohexylamine, 3.23 g (4.36 mL, 25.0 mmol) of diisopropylethylamine, and 100 mL of THF. The solution was heated at reflux for 5 h under a nitrogen atmosphere and then cooled to room temperature, and the solvent was removed by rotary evaporation at aspirator pressure. The residue was taken up in 500 mL of ethyl acetate, washed four times with 300-mL portions of water and once with 150 mL of brine, and dried over $MgSO_4$, and the solvent was removed by rotary evaporation at aspirator pressure. The product was purified by flash chromatography (eluted with ethyl acetate, loaded on a column preadsorbed to silica) to give 4.14 g (9.94 mmol, 84%) of the product as a white solid: ^{1}H NMR (400 MHz, DMSO-d_6) δ 10.22, 10.16 (two conformers, s, 1 H), 8.86 (m, 1 H), 7.76 (s, 1 H), 7.35, 7.30 (two conformers, d, J = 8.6 Hz, 1 H), 6.95

(s, 1 H), 6.61 (br s, 1 H), 6.45 (br s, 1 H), 4.52 (t, J = 5.1 Hz, 1 H), 4.30 (t, J = 6.5 Hz, 2 H), 3.46 (m, 2 H), 3.29 (m, 2 H), 2.29 (s, 3 H), 1.76 (m, 2 H), 1.56 (m, 2 H), 1.44 (m, 2 H), 0.95, 0.92 (two conformers, s, 9 H); ^{13}C NMR (100 MHz, DMSO-d_6) δ 167.62, 167.05, 166.69, 165.97, 165.78, 164.26, 163.93, 140.73, 140.59, 134.70, 134.44, 130.44, 129.00, 128.82, 124.88, 119.95, 113.93, 113.65, 64.87, 60.32, 43.14, 42.68, 36.56, 30.39, 29.52, 29.34, 28.98, 24.98, 20.12; HRMS-FAB (M + H$^+$) calcd for $C_{21}H_{33}N_6O_3$ 417.2614, found 417.2624.

***h*-flexM′$_3$.** A 100-mL round-bottomed flask equipped with a stirring bar was charged with 2.08 g (5.0 mmol) of alcohol **14**, 0.71 g (0.96 mL, 5.5 mmol) of diisopropylethylamine, and 40 mL of THF. The solution was cooled in an ice bath under a nitrogen atmosphere, 0.44 g (1.67 mmol) of 1,3,5-benzenetricarboxylic acid chloride was added, and the solution was stirred at 0 °C for 2 h and at room temperature for 12 h. The solvent was removed by rotary evaporation at aspirator pressure and the residue was taken up in 300 mL of ethyl acetate. The organic layer was washed twice with 150-mL portions of water, twice with 100-mL portions of saturated aqueous sodium carbonate solution, twice with 150-mL portions of water, and once with 100 mL of brine and dried over $MgSO_4$, and the solvent was removed by rotary evaporation at aspirator pressure. The crude product was purified by flash chromatography (eluted with ethyl acetate followed by 97:3 ethyl acetate/methanol, loaded on a column preadsorbed to silica) to give 1.08 g (0.77 mmol, 46%) of the product as a white foam: ^{1}H NMR (400 MHz, DMSO-d_6) δ 10.21, 10.15 (two conformers, s, 3 H), 8.85, 8.77 (two conformers, d, J = 8.5 Hz, 3 H), 8.50 (br s, 3 H), 7.70 (s, 3 H), 7.29, 7.18 (two conformers, d, J = 8.4 Hz, 3 H), 6.93 (m, 3 H), 6.62 (br s, 3 H), 6.45 (br s, 3 H), 4.37 (br s, 12 H), 3.28 (br s, 6 H), 2.23 (s, 9 H), 1.92 (br s, 12 H), 1.45 (br s, 6 H), 0.93 (br s, 27 H); ^{13}C NMR (100 MHz, DMSO-d_6) δ 167.46, 167.01, 166.65, 165.91, 165.74, 164.16, 163.88, 140.74, 140.62, 134.64, 134.35, 133.13, 130.69, 130.31, 128.75, 128.65, 119.76, 113.52, 113.36, 65.03, 64.42, 43.11, 42.64, 36.50, 29.28, 24.93, 24.78, 20.01; HRMS-FAB (M + Na$^+$) calcd 1427.7352, found 1427.7380. Anal. Calcd for $C_{72}H_{96}N_{18}O_{12}$: C, 61.52; H, 6.88; N, 17.94. Found: C, 61.57; H, 6.95; N, 17.89.

NOE Spectra of *h*-flexM$_3$·hubCA$_3$. The NOE spectra of *h*-flexM$_3$·hubCA$_3$ were recorded at 25 °C. The complex (5.0 μmol) was dissolved in 0.5 mL of $CDCl_3$, and the sample was degassed with five freeze–pump–thaw cycles. The NOE spectra were collected with an evolution period of 3.0 s and a relaxation delay of 6.0 s.

Gel Permeation Chromatography. Gel permeation chromatography was performed using a Waters 600E HPLC with a Waters 484 UV detector and Waters analytical gel permeation column (Ultrastyragel, 1000 Å pore size). Elutions were performed at room temperature using HPLC-grade $CHCl_3$ (stabilized with amylenes rather than ethanol) as the solvent at a flow rate of 1.0 mL/min. The samples were prepared at a concentration of 0.25 mM in $CHCl_3$ that contained *p*-xylene (3.0 mM) as an internal reference. The injection volume was 20 μL.

Molecular Weight Determinations of *h*-flexM$_3$·hubCA$_3$ by Vapor Pressure Osmometry. Molecular weight determinations were made with a Wescan Model 233 vapor pressure osmometer operated at 35 °C. The molecular weights of the complexes were measured in HPLC-grade glass-distilled chloroform at concentrations of approximately 2, 4, 8, and 16 mM. At each concentration, 3–4 measurements were taken. Calibration curves were generated using sucrose octaacetate (Aldrich), perbenzoyl β-cyclodextrin,[28] polystyrene (MW 5050, polydispersity = 1.05) (Polymer Laboratories), and a gramicidin S derivative in which the ornithine amino groups had been converted to the *tert*-butylcarbamates[1] (MW 1342) as molecular weight standards.

Exchange between *h*-flexM$_3$·hubCA$_3$ and *h*-flexM′$_3$ Monitored by ^{1}H NMR Spectroscopy. Samples for the variable-temperature experiments were prepared at 5 mM concentrations of [*h*-flexM$_3$·hubCA$_3$]$_0$ and [*h*-flexM′$_3$]$_0$. An NMR tube was charged with 10.3 mg of *h*-flexM$_3$·hubCA$_3$, 3.5 mg of *h*-flexM′$_3$, and 0.5 mL of $CDCl_3$, and the tube was flame sealed. For the experiments that were performed at 40, 55, and 70 °C, the temperature was maintained in a stirred oil bath equipped with a temperature regulator. The experiment at 25 °C was performed at ambient temperature. ^{1}H NMR spectra of the samples were taken at periodic intervals on a Bruker AM 500 spectrometer, and the progress of the reaction was followed by integration of the resonance at 7.66 ppm with respect to the resonance at 8.09 ppm. Integrations were performed by plotting the spectrum, estimating a base line, and cutting out and weighing the appropriate resonances. The relative weights of the areas of the two resonances were used as a measure of the progress of the reaction.

The experiments performed at variable concentrations were maintained at 22 °C in a temperature-controlled water-circulating bath located in a cold room in which the ambient temperature was 4 °C. The reactions were performed at the following concentrations: ratio [*h*-flexM$_3$·hubCA$_3$]$_0$:[*h*-flexM′$_3$]$_0$ = 1:1, [*h*-flexM$_3$·hubCA$_3$]$_0$ = 5 mM, [*h*-flexM′$_3$]$_0$ = 5 mM; ratio = 1:4, [*h*-flexM$_3$·hubCA$_3$]$_0$ = 5 mM, [*h*-flexM′$_3$]$_0$ = 20 mM; ratio = 1:10, [*h*-flexM$_3$·hubCA$_3$]$_0$ = 2.5 mM, [*h*-flexM′$_3$]$_0$ = 25 mM. For the experiment at a 1:10 ratio, the concentration of [*h*-flexM$_3$·hubCA$_3$]$_0$ was lowered to 2.5 mM because *h*-flexM′$_3$ was difficult to solubilize at high concentrations.

The preformed *h*-flexM$_3$·hubCA$_3$ complex was prepared by dissolving the components in $CHCl_3$ (the hubCA$_3$ was slow to dissolve) and stirring the mixture for ~24 h. The solvent was removed by rotary evaporation at aspirator pressure, and the resulting solid was dried for several hours in an oven at 80 °C.

Acknowledgment. This work was supported by the National Science Foundation (Grants CHE-91-22331 to G.M.W. and DMR 89-20490 to the Harvard University Materials Research Laboratory). C.T.S. was an Eli Lilly Predoctoral Fellow, 1991. NMR instrumentation was supported by National Science Foundation Grant CHE-88-14019 and National Institutes of Health Grant 1 S10 RR4870. Mass spectra were obtained by Dr. Andrew Tyler. The Harvard University Chemistry Department Mass Spectrometry Facility was supported by National Science Foundation Grant CHE-90-20043 and National Institutes of Health Grant 1 S10 RR06716-01. We thank Professor Robert Cohen (Department of Chemical Engineering, MIT) for lending us his vapor pressure osmometer.

(28) Boger, J.; Corcoran, R.; Lehn, J. M. *Helv. Chim. Acta* **1978**, *61*, 2190.